AN INTEGRATED USED FUEL DISPOSITION AND GENERIC REPOSITORY MODEL

by

Kathryn D. Huff

A dissertation submitted in partial fulfillment of
the requirements for the degree of

Doctor of Philosophy

(Nuclear Engineering and Engineering Physics)

at the

UNIVERSITY OF WISCONSIN–MADISON

2011

© Copyright by Kathryn D. Huff 2011

All Rights Reserved

ACKNOWLEDGMENTS

I am grateful to a number of extraordinary professors and colleagues at the Universities of Wisconsin and Chicago who have inspired and encouraged me. Among them, I am especially indebted to my advisor, Paul P.H. Wilson, for his invaluable technical and practical guidance. I am also grateful to my laboratory advisor, Mark Nutt, and laboratory collaborator, Ted Bauer. They have been an outstanding resource for the work at hand and I look forward to learning a great deal from them in the upcoming phase of my research.

LIST OF TABLES

LIST OF FIGURES

AN INTEGRATED USED FUEL DISPOSITION AND GENERIC REPOSITORY MODEL

Kathryn D. Huff

Under the supervision of Professor Paul P.H. Wilson
At the University of Wisconsin-Madison

As the United States Department of Energy (DOE) simultaneously considers alternative fuel cycles and waste disposal options, an integrated fuel cycle and generic disposal system analysis tool is increasingly necessary for informing domestic nuclear spent fuel policy. A generic repository model capabable of illuminating the distinct dominant physics of candidate repository geologies, designs, and engineering components will provide an interface between the Used Fuel Disposition (UFD) and Fuel Cycle Options (FCO) Campaign goals. Repository metrics such as necessary repository footprint and peak annual dose are affected by heat and radionuclide release characteristics specific to variable spent fuel compositions associated with alternative fuel cycles. Computational tools capable of simulating the dynamic, heterogeneous spent fuel isotopics resulting from transition scenarios and alternative fuel cycles are, however, lacking in repository modeling options. This work proposes to construct such a generic repository model appropriate for systems analysis. By emphasizing modularity and speed, the work at hand seeks to provide a tool which captures the dominant physics of detailed repository analysis within the UFD Campaign and can be robustly and flexibly integrated within the Cyclus fuel cycle simulation tool.

Paul P.H. Wilson

ABSTRACT

As the United States Department of Energy (DOE) simultaneously considers alternative fuel cycles and waste disposal options, an integrated fuel cycle and generic disposal system analysis tool is increasingly necessary for informing domestic nuclear spent fuel policy. A generic repository model capabable of illuminating the distinct dominant physics of candidate repository geologies, designs, and engineering components will provide an interface between the Used Fuel Disposition (UFD) and Fuel Cycle Options (FCO) Campaign goals. Repository metrics such as necessary repository footprint and peak annual dose are affected by heat and radionuclide release characteristics specific to variable spent fuel compositions associated with alternative fuel cycles. Computational tools capable of simulating the dynamic, heterogeneous spent fuel isotopics resulting from transition scenarios and alternative fuel cycles are, however, lacking in repository modeling options. This work proposes to construct such a generic repository model appropriate for systems analysis. By emphasizing modularity and speed, the work at hand seeks to provide a tool which captures the dominant physics of detailed repository analysis within the UFD Campaign and can be robustly and flexibly integrated within the Cyclus fuel cycle simulation tool.

1 INTRODUCTION

The scope of this work includes implementation of a software library of medium fidelity models to comprehensively represent various long-term disposal system concepts for nuclear material. This software library will be integrated with a computational fuel cycle systems analysis platform in order to inform repository performance metrics with respect to candidate fuel cycle options. By abstraction of more detailed models, this work will capture the dominant physics of radionuclide and heat transport phenomena affecting repository performance in various geologic media and as a function of arbitrary spent fuel composition.

1.1 Motivation

The development of sustainable nuclear fuel cycles is a key challenge as the use of nuclear power expands domestically and internationally. While fuel cycle performance may be measured with respect to a variety of metrics, waste management metrics are of particular importance to the goal of sustainability. Since disposal options are influenced by upstream fuel cycle decisions, a relevant analysis of potential geological disposal and engineered barrier solutions requires a system level approach that is both modular and efficient.

As the merits of numerous combinatoric fuel cycle possibilities are investigated, a top-level simulation tool capable of modular substitution of various fuel cycle facility, repository, and engineered barrier components is needed. The modular waste package and repository models resulting from this work will assist in informing current technology choices, identifying important parameters contributing to key waste disposal metrics, and highlighting the most promising waste disposal combinations with respect

to metrics chosen by the user. Specifically, such models will support efforts underway in focusing domestic research and development priorities as well as computational tools under development that quantify these metrics and demonstrate the merits of different fuel cycle alternatives.

System level fuel cycle simulation tools must facilitate efficient sensitivity and uncertainty analyses as well as simulation of a wide range of fuel cycle alternatives. Efficiency is achieved with models at a level of detail that successfully captures significant aspects of the underlying physics while achieving a calculation speed in accordance with use cases requiring repeated simulations. Often termed abstraction, the process of simplifying while maintaining the salient features of the underlying physics is the method by which used fuel disposal system models will be developed in this work.

Independent fuel cycle parameters of particular interest in fuel cycle systems analysis have been those related to the front end of the fuel cycle. Deployment decisions concerning reactor types, fast to thermal reactor ratios, and burnup rates can all be independently varied in fuel cycle simulation codes in such a way as to inform domestic policy decisions going forward. Some of these parameters are coupled, however, to aspects of the back end of the fuel cycle. For example, the appropriate fast reactor ratio is significantly altered by the chosen method and magnitude of domestic spent fuel reprocessing (or not).

However, independent variables representing decisions concerning the back end of the fuel cycle are of increasing interest as the United States further investigates repository alternatives to Yucca Mountain. Parameters such as the repository geology, engineered barriers, appropriate loading strategies and schedules are all independent variables up for debate. All of these parameters are coupled with decisions about the fuel cycle.

Thus, while independent parameters can be chosen and varied within a fuel cycle

simulation, some parameters are coupled in such a way as to require full synthesis with a systems analysis code that appropriately determines the isotopic mass flows into the repository, their appropriate conditioning, densities, and other physical properties.

Future Fuel Cycle Options

Domestically, nuclear power expansion is motivated by the research, development, and demonstration roadmap being pursued by the United States Department of Energy Office of Nuclear Energy (DOE-NE), which seeks to ensure that nuclear energy remain a viable domestic energy option [**?**].

As the DOE-NE seeks to develop technologies and strategies to support a sustainable future for nuclear energy, various fuel cycle strategies and corresponding disposal system options are being considered. Specifically, the domestic fuel cycle option space under current consideration is described in terms of three distinct fuel cycle categories with the monikers Once Through, Full Recycle, and Modified Open. Each category presents unique disposal system siting and design challenges. Systems analyses for evaluating these options must be undertaken in order to inform a national decision to deploy a comprehensive fuel cycle system by 2050 [**?**].

The Once-Through Cycle category includes fuel cycles similar to the continuation of the business as usual case in the United States. Such fuel cycles neglect reprocessing and present challenges associated with high volumes of minimally treated spent fuel streams. In a business as usual scenario, conventional power reactors comprise the majority of nuclear energy production and fuel takes a single pass through a reactor before it is classified as waste and disposed of. In the open cycle, no reprocessing is pursued, but research and development of advanced fuels seek to reduce waste volumes. Calculations from the Electric Power Research Institute corroborated by the United

States (US) Department of Energy (DOE) in 2008 indicate that without an increase in the statutory capacity limit of the Yucca Mountain Repository Site (YMR), continuation of the current Once Through fuel cycle will generate a volume of spent fuel that will necessitate the siting of an additional federal geological repository to accommodate spent fuel [**? ?**].

A Full Recycle option, on the other hand, requires the research, development, and deployment of partitioning, transmutation, and advanced reactor technology for the reprocessing of used nuclear fuel. In this scheme, conventional once-through reactors will be phased out in favor of fast reactor and so called Generation IV reactor technologies, which demonstrate transmutation capacity and greater fuel efficiency. All fuel in the Full Recycle strategy will be reprocessed. It may be reprocessed using an accelerator driven system or by cycling through an advanced fast reactor. Such fuel may undergo partitioning, the losses from which will require waste treatment and ultimate disposal in a repository. Thus, a repository under the Full Recycle scenario must support a waste stram composition that is highly variable during transition periods as well as myriad waste forms and packaging associated with isolation of differing waste streams.

Finally, the Modified Open Cycle category of options includes a variety of fuel cycle options that fall between once through and fully closed. Advanced fuel cycles such as deep burn and small modular reactors will be considered within the Modified Open set of fuel cycle options as will partial recycle options. Partitioning and reprocessing strategies, however, will be limited to simplified chemical separations and volatilization under this scheme. This scheme presents a dual challenge in which spent fuel volumes and composition will both vary dramatically among various possibilities within this scheme [**?**] .

Clearly, the myriad waste streams resulting from potential fuel cycles present an

array of corresponding waste disposition, packaging, and engineered barrier system options. For a comprehensive analysis of the disposal system, dominant physics models must therefore be developed for each of these subcomponents. Differing spent fuel composition, partitioning, transmutation, and chemical processing decisions upstream in the fuel cycle demand differing performance and loading requirements of waste forms and packaging. The capability to model thermal and radionuclide transport phenomena through, for example, vitrified glass as well as ceramic waste forms with with various loadings for arbitrary isotopic compositions is therefore required. This work will produce a repository model that meets this need.

Future Waste Disposal System Options

In addition to reconsideration of the domestic fuel cycle policy, the uncertain future of the YMR has driven the expansion of the option space of potential repository host geologies to include, at the very least, granite, clay/shale, salt, and deep borehole concepts [**?**].

In accordance with various fuel cycle options, corresponding waste form, waste package, and other engineered barrier systems are being considered. Specifically, current considerations include ceramic (e.g. Uranium Oxide), glass (e.g. borosilicate glasses), and metallic (e.g. hydride fuels) waste forms. Waste packages may be copper, steel, or other alloys. Similarly, buffer and backfill materials vary from the crushed salt recommended for a salt repository to bentonite or concrete in other geologies. Therefore, a repository model capable of modular substitution of waste form models and data will be necessary to analyze the full option space.

The physical, hydrologic, and geochemical mechanisms that dictate radionuclide and heat transport vary between the geological and engineered containment systems in the domestic disposal system option space. Therefore, in support of the system level

simulation effort, models must be developed that capture the salient physics of these geological options and quantify associated disposal metrics and benefits. Furthermore, in the same way that system level modularity facilitates analysis, so too will modular linkage between subcomponent process modules. These subcomponent models and the repository environmental model must achieve a cohesively integrated disposal system model such as is proposed by this work.

Thermal Modeling Needs

The decay heat from nuclear material generates a significant heat source within a repository. In order to arrive at loading strategies that comply with thermal limits in the engineered barrier system and the geological medium, a thermal modeling capability must be included in the repository model. Such a model is also necessary to inform material and hydrologic phenomena that affect radionuclide transport and are thermally coupled.

Partitioning and transmutation of heat generating radionuclides within some fuel cycles will alter the heat evolution of the repository [**?**]. Thus, to distinguish between the repository heat evolution associated with various fuel cycles involving partitioning and transmutation, a repository analysis model, must at the very least, capture the decay heat behavior of dominant heat contributors. Plutonium, Americium, and their decay daughters dominate decay heat contribution within used nuclear fuels. Other contributing radionuclides include Cesium, Strontium, and Curium [**?**].

Thermal limits within a used nuclear fuel disposal system are waste form, package, and geology dependent. The heat evolution of the repository constrains waste form loadings and package loadings as heat generated in the waste form is transported through the package. It also places requirements on the size, design, and loading

strategy in a potential geological repository as that heat is deposited in the engineered barrier system and host geology.

Thermal limits of various waste forms have their technical basis in the temperature dependence of isolation integrity of the waste form. Waste form alteration, degradation, and dissolution behavior is a function of heat in addtition to redox conditions and constrains loading density within the waste form.

Thermal limits of various engineered barrier systems similarly have a technical basis in the temperature dependent alteration, corrosion, degradation, and dissolution rates of the materials from whence they are constructed.

Thermal limits of the geologic environment can be based on the mechanical integrity of the rock as well as mineralogical, hydrologic and geochemical phenomena. The isolating characteristics of a geological environment are most sensitive to hydrologic and geochemical effects of thermal loading. Thus, heat load constraints are typically chosen to control hydrologic and geochemical response to thermal loading. In the United States, current regulations necessitate thermal limits in order to passively steward the repository's hydrologic and geochemical integrity against radionuclide release for the first 10,000 years of the repository.

The two heat load constraints that primarily determined the heat-based spent nuclear fuel (SNF) capacity limit in the Yucca Mountain Repository design, for example, are specific to unsaturated tuff. These are given here as an example of the type of regulatory constraints that this model will seek to capture for various geologies.

The first Yucca Mountain heat load constraint is intended to promote constant drainage, thereby preventing episodic flow into waste package tunnels and subsequent contaminated water flow through the repository. It requires that the minimum temperature in the tuff between drifts be no more than the boiling temperature of water,

which is $96°C$ at the altitude in question. For a repository with homogeneous waste composition in parallel drifts, this constraint limits the temperature exactly halfway between adjacent drifts, where the temperature is at a minimum.

The second constraint is intended to prevent high rock temperatures that could induce fractures and alteration of the rock. It stated that no part of the rock reach a temperature above $200°C$, and was effectively a limit on the temperature at the drift wall, where the rock temperature is a maximum.

Analogous constraints for a broader set of possible geological environments will depend on heat transport properties and geochemical behaviors of the rock matrix as well as its hydrologic state. Such constraints will affect the repository drift spacing, waste package spacing, and repository footprint among other parameters.

In addition to development of a concept of heat transport within the repository in order to meet heat load limitations, it is also necessary to model temperature gradients in the repository in order to support modeling of thermally dependent hydrologic and material phenomena. As mentioned above, waste form corrosion processes, waste form dissolution rates, diffusion coefficients, and the mechanical integrity of engineered barriers and geologic environment are coupled with temperature behavior. Only a coarse time resolution will likely be necessary to capture that coupling however, since time evolution of repository heat is such that thermal coupling can typically be treated as quasi static for long time scales. [**?**].

Source Term Modeling Needs

Domestically, the Environmental Protection Agency (EPA) has defined a limit on human exposure due to the repository. This regulation places important limitations on capacity, design, and loading techniques for repository concepts under consideration. Repository

concepts developed in this work must therefore quantify radionuclide transport through the geological environment in order to calculate repository capacity and other benefit metrics.

The exposure limit set by the EPA is based on a 'reasonably maximally exposed individual.' For the YMR, the limiting case is a person who lives, grows food, drinks water and breathes air 18 km downstream from the repository. The Yucca Mountain Repository EPA regulations limit total dose from the repository to 15 mrem/yr, and limit dose from drinking water to 4 mrem/yr for the first 10,000 years. Predictions of that dose rate depend on an enormous variety of factors, most important of which is the primary pathway for release. In the YMR primary pathway of radionuclides from an accidental release will be from cracking aged canisters. Subsequently, transport of the radionuclides to the water table requires that the radionuclides come in contact with water and travel through the rock to the water table. This results in contamination of drinking water downstream.

Source term is a measure of the quantity of a radionuclide released into the environment whereas radiotoxicity is a measure of the hazardous effect of that particular radionuclide upon human ingestion or inhalation. In particular, radiotoxicity is measured in terms of the volume of water dilution required to make it safe to ingest. Studies of source term and radiotoxicity therefore make probabilistic assessments of radionuclide release, transport, and human exposure.

Importantly, due to the long time scale and intrinsic uncertainties required in such probabilistic assessments it is in general not advisable to base any maximum repository capacity estimates on source term. This is due to the fact that in order to give informative values for the risk associated with transport of particular radionuclides, for example, it is necessary to make highly uncertain predictions concerning waste form degradation, wa-

ter flow, and other parameters during the long repository evolution time scale. However, source term remains a pertinent metric for the comparison of alternative separations and fuel cycle scenarios as it is a fundamental factor in the calculation of risk.

Arriving at a generalized metric of probabilistic risk is fairly difficult. For example, the Peak Environmental Impact (PEI) metric from Berkeley (ref. [**?**]) is a multifaceted function of spent fuel composition, waste conditioning, vitrification method, and radionuclide transport through the repository walls and rock. Also, it makes the assumption that the waste canisters have been breached at $t = 0$. Furthermore, reported in m^3, PEI is a measure of radiotoxicity in the environment in the event of total breach. While informative, this model on its own does not completely determine a source-term limited maximum repository capacity. Additional waste package failure and a dose pathway model must be incorporated into it.

Domestic Research and Development Program

The DOE-NE Fuel Cycle Technology (FCT) program has three groups of relevance to this effort: these are the Used Fuel Disposition (UFD), the Separations and Waste Forms (SWF), and Fuel Cycle Options (FCO) (previously Systems Analysis) campaigns. The UFD campaign is conducting the Research Development and Design (RD&D) related to the storage, transportation, and disposal of radioactive wastes generated under both the current and potential advanced fuel cycles. The SWF campaign is conducting RD&D on potential waste forms that could be used to effectively isolate the wastes that would be generated in advanced fuel cycles. The SWF and UFD campaigns are developing the fundamental tools and information base regarding the performance of waste forms and geologic disposal systems. The FCO campaign is developing the overall fuel cycle simulation tools and interfaces with the other FCT campaigns, including UFD.

This effort will interface with those campaigns to develop the higher level dominant physics representations for use in fuel cycle system analysis tools. Specifically, this work will leverage conceptual framework development and primary data collection underway within the Used Fuel Disposition Campaign as well as work by Radel, Wilson, Bauer et. al. to model repository behavior as a function of the contents of the waste [**?**]. It will then incorporate dominant physics process models into the Cyclus computational fuel cycle analysis tool [**?**].

1.2 Methodology

In this work, concise dominant physics models suitable for system level fuel cycle codes will be developed by comparison of analytical models with more detailed repository modeling efforts. The ultimate objective of this effort is to develop a software library capable of assessing a wide range of combinations of fuel cycle alternatives, potential waste forms, repository design concepts, and geological media.

Current candidate repository concepts have been investigated and reviewed here in order to arrive at a fundamental set of components to model. A preliminary set of combinations of fuel cycles, repository concepts, and geological environments has been chosen that fundamentally captures the domestic option space. Specifically, three candidate geologies and four corresponding repository concepts under consideration by the DOE UFD campaign have been chosen for modeling in this work. These will be expected to interface with Cyclus simulations of a canonical set of potential fuel cycles within three broad candidate scenarios put forth by the US DOE.

A review and characterization of the physical mechanisms by which radionuclide and thermal transport take place within the materials and media under consideration was first undertaken. Potential analytical models to represent these phenomena were

investigated and categorized within the literature review.

A review and characterization of current detailed computational tools for repository focused analysis was next conducted. Both international and domestic repository modeling efforts were summarized within the literature review. Of these, candidate computational tools with which to perform abstraction and regression analyses were identified. Specifically, a suite of Generic Disposal System Model (GDSM) tools under development by the DOE UFD campaign will inform radionuclide transport models and a pair of corresponding thermal analysis codes will inform the thermal models.

Continuation of this work will consist of the development of a suite of subcomponent modules appropriate for use within the Cyclus fuel cycle simulator. This process will include the development of a robust architecture within the repository module that will allow for interchangeable loading of system components. Within the system components, dominant physics will be modeled based on domain appropriate approximation of analytical models and supported by abstraction with the chosen GDSM tools and thermal tools.

In general, such concise models are a combination of two components: semi-analytic mathematical models that represent a simplified description of the most important physical phenomena, and semi-empirical models that reproduce the results of detailed models. By combining the complexity of the analytic models and regression against numerical experiments, variations can be limited between two models for the same system. Different approaches will be compared in this work, with final modeling choices balancing the accuracy and efficiency of the possible implementations.

Specifically, geological models will focus on the hydrology and thermal physics that dominate radionuclide transport and heat response in candidate geologies as a function of radionuclide release and heat generation over long time scales. Dominant

transport mechanism (advection or diffusion) and disposal site water chemistry (redox state) will provide primary differentiation between the different geologic media under consideration. In addition, the concise models will be capable of roughly adjusting release pathways according to the characteristics of the natural system (both the host geologic setting and the site in general) and the engineered system (such as package loading arrangements, tunnel spacing, and engineered barriers).

The abstraction process in the development of a geological environment model will employ the comparison of semi-analytic thermal and hydrologic models and analytic regression of rich code results from more detailed models as well as existing empirical geologic data. Such results and data will be derived primarily from the UFD campaign GDSMs and data, as well as European efforts such as the RED-IMPACT assessment and Agence Nationale pour la gestion des Déchets RAdioactifs, the French National Agency for Radioactive Waste Management (ANDRA) Dossier efforts [**? ? ?**] .

Thereafter, a regression analysis concerning those parameters will be undertaken with available detailed models (e.g. 2D and 3D finite difference, finite element, and thermal performance assessment codes) to further characterize the parametric dependence of thermal loading in a specific geologic environment.

Finally, the thermal behavior of a repository model so developed will depend on empirical data (e.g. heat transfer coefficients, hydraulic conductivity). Determination of representative values to make available within the dominant physics model will rely on existing empirical data concerning the specific geologic environment being modeled (i.e. salt, clay/shale, and granite).

A similar process will be followed for radionuclide transport models. The abstraction process in the development of waste form, package, and engineered barrier system models will be analogous to the abstraction process of repository

environment models. Concise models will result from employing the comparison of semi-analytic models of those systems with regression analysis of rich code in combination with existing empirical material data.

Coupling effects between components will have to be considered carefully. In particular, given the important role of temperature in the system, thermal coupling between the models for the engineered system and the geologic system may be important. Thermal dependence of radionuclide release and transport as well as package degradation will necessarily be analyzed to determine the magnitude of coupling effects in the system.

The full abstraction process will be iterated to achieve a balance between calculation speed and simulation detail. Model improvements during this stage will seek a level of detail appropriate for informative comparison of subcomponents, but with sufficient speed to enable systems analysis.

By varying input parameters and comparing with corresponding results from detailed tools, each model's behavior on its full parameter domain will be validated.

1.3 Outline

The following chapter will present a literature review that organizes and reports upon previous relevant work. First it summarizes the state of the art of repository modeling integration within current systems analysis tools. It then describes current domestic and international disposal system concepts and geologies. Next, the literature review focuses upon current analytical and computational modeling of radionuclide and heat transport through various waste forms, engineered barrier systems, and geologies of interest. It will also address previous efforts in generic geologic environment repository modeling in order to categorize and characterize detailed computational models of radionuclide and heat transport available for regression analysis.

Chapter **??** will detail the computational paradigm of the Cyclus systems analysis platform and repository model which constitute this work. Models representing waste form, waste package, buffer, backfill, and engineered barrier systems will be defined by their interfaces and their relationships as interconnected modules, distinctly defined, but coupled. This modular paradigm allows exchange of technological options (i.e. borosilicate glass and concrete waste forms) for comparison but also exchange of models for the same technological option with varying levels of detail.

Chapter **??** will summarize the conclusions reached concerning the appropriate analytical and detailed models to utilize in the process of abstraction for radionuclide and heat transport through various components of the disposal system. It will then detail the analytical and regression analysis necessary to achieve a generic repository model for the chosen base repository type. A concise, dominant physics geological repository model of the base case disposal environment will be developed. Informed by semi-analytic mathematical models representing important physical phenomena, existing detailed computational efforts characterizing these repository environments will be appropriately simplified to create concise computational models. This abstraction will capture fundamental physics of thermal, hydrologic, and radionuclide transport phenomena while remaining sufficiently detailed to illuminate behavioral differences between each of the geologic systems under consideration. Verification and validation of abstracted models will be conducted through iterative benchmarking against more detailed repository models. Finally, remaining future work and expected contributions to the field will be summarized.

2 MODELING PARADIGM

The modeling paradigm with which this repository model and simulation platform are implemented are described here. Implications of the simulation platform architecture on the design of the repository model are discussed and the interfaces defining components of the repository model follow.

2.1 Cyclus Simulator Paradigm

The Cyclus project at the University of Wisconsin (UW) at Madison is the simulation framework in which this repository model is designed to operate. Modular features within this software architecture provide a great deal of flexibility, both in terms of modifying the underlying modeling algorithms and exchanging components of a fuel cycle system.

The Cyclus fuel cycle simulator is the result of lessons learned from experience with previous nuclear fuel cycle simulation platforms. The modeling paradigm follows the transaction of discrete quanta of material among discrete facilities, arranged in a geographic and institutional framework, and trading in flexible markets. Key concepts in the design of Cyclus include open access to the simulation engine, modularity with regard to functionality, and relevance to both scientific and policy analyses. The combination of modular encapsulation within the software architecture and dynamic module loading allows for robust but flexible reconfiguration of the basic building blocks of a simulation without alteration of the simulation framework.

The modeling paradigm adopted by Cyclus includes a number of fundamental concepts that comprise the foundation on which other, more flexible, design choices have been made.

Dynamic Module Loading

The ability to dynamically load independently constructed modules is a heavy focus of Cyclus development. Dynamically-loadable modules are the primary mechanism for extending Cyclus ' capability. The primary benefit of this approach is encapsulation: the trunk of the code is completely independent of the individual models. Thus, any customization or extension is implemented only in the loadable module. A secondary benefit of this encapsulation is the ability for contributors to choose different distribution and licensing strategies for their contributions. By allowing models to have varied availability, the security concerns of developers can be assuaged (See Figure **??**).

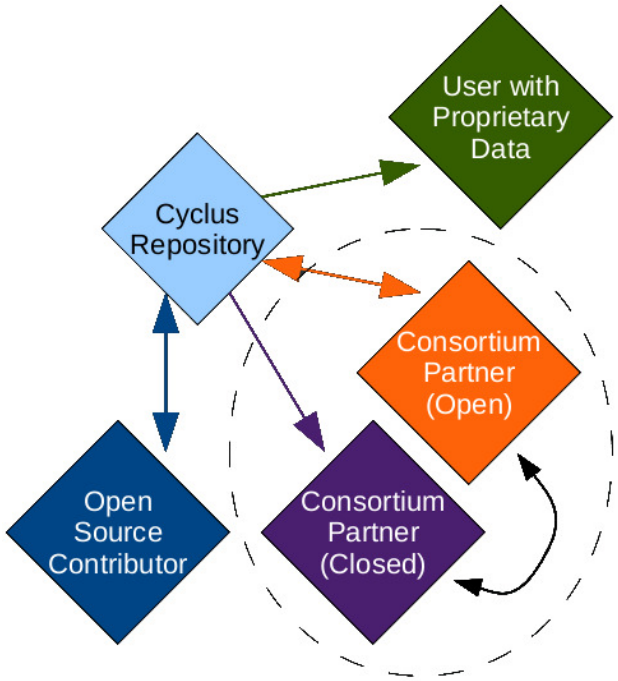

Figure 2.1: The Cyclus code repository allows for varied accessibility.

Finally, this strategy allows individual developers to explore different levels of complexity within their modules, including wrapping other simulation tools as loadable modules within the Cyclus framework. This last benefit of dynamically-loadable mod-

ules addresses another goal of Cyclus : ubiquity amongst its potential user base. By engineering Cyclus to easily handle varying levels of complexity, a single simulation engine can be used by both users keen on big-picture policy questions as well as users interested in more detailed, technical analyses.

Encapsulation

Cyclus implements an encapsulated structure that takes advantage of object-oriented software design techniques in order to create an extensible and modular user and developer interface. A primary workhorse for this implementation is the notion of dynamic module loading in combination with well defined module interfaces within a region, institution, and facility hierarchy. In this paradigm, the shared interface of polymorphic objects is abstracted from the logic of their instantiation by the model definition they inherit.

In this way, Cyclus allows a level of abstraction to exist between the simulation and model instantiation as well as between model instantiation and behavior. An interface defines the set of shared functions of a set of subclasses in an abstract superclass. In Cyclus main superclasses are Regions, Institutions, Facilities, and Markets while their subclasses are the concrete available model types (e.g. a RecipeReactorFacility). See Figure **??**.

The interface for the FacilityModel class is the set of virtual functions declared in the Facility class such as getName, getID, executeOrder(), sendMaterial(), receiveMaterial() etc. Through such an interface, the members of a subclass can be treated as interchangeable (polymorphic) instantiations of their shared superclass.

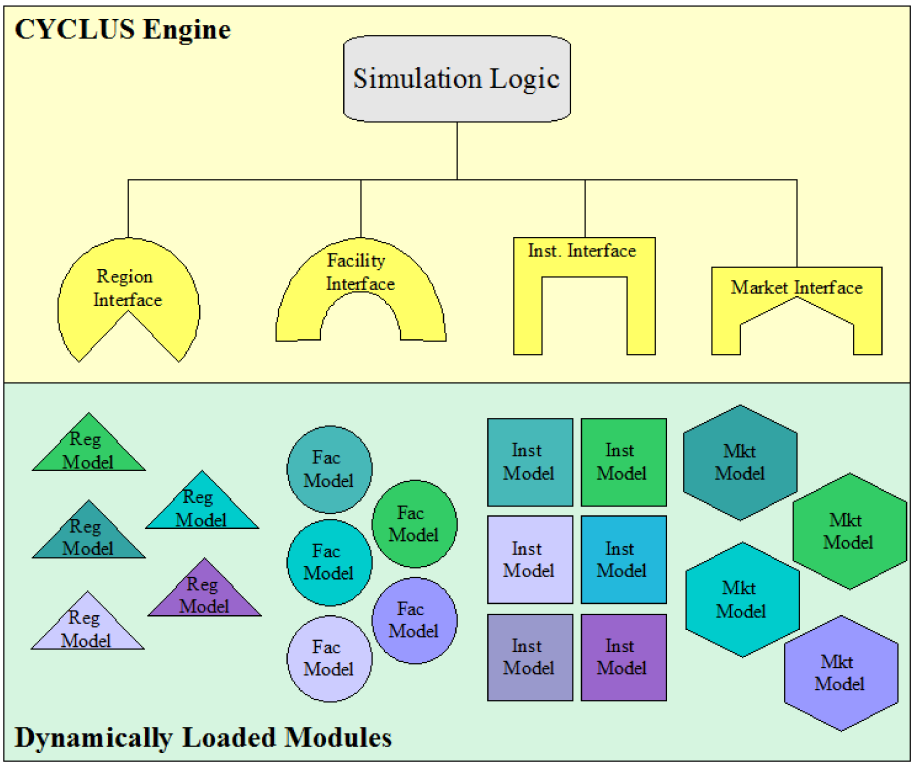

Figure 2.2: Modules are defined solely by their interfaces in a modular paradigm and can be arbitrarily interchanged with modules posessing equivalent interfaces.

Modularity and Extensibility

A modular code must have the traits of encapsulation and abstraction appropriate for a user or developer to flexibly make alterations to the simulation performance with minimal modification to the code. An extensible code should be both robustly suited to the addition of classes and subclasses as well as suited to communication with other codes. In Cyclus , addition of new models by dynamic loading is possible without any alteration of the software trunk. The modular design of Cyclus stresses avoidance of rigidity, in which changes to the code are potentially difficult, and fragility, in which changes to the code are potentially damaging.

Market-based Material Transactions

The foundation of a simulation is a commodity market that collects offers and requests and matches them according to some algorithm. The user is able to select which type of algorithm is used for each market by selecting a MarketModel and configure it with a particular set of parameters defined by that MarketModel. Changing the parameters of a market changes its performance and selecting a different MarketModel completely changes its behavior.

The transaction of nuclear materials takes place in markets that act as brokers matching a set of requests for material with a set of offers for that material. A variety of market models will be available to perform this brokerage role. It is important to note that each market is defined for a single commodity and acts independently of other markets. Once the requests and offers have been matched by each market in a simulation, the facilities exchange material objects.

Facilities are deployed to issue offers and requests in these markets. Like markets, the user may select which type of algorithm is used for each facility by selecting a FacilityModel and configure it with a particular set of parameters defined by that FacilityModel. Changing the parameters of a facility changes its performance and selecting a different FacilityModel completely changes its behavior. Unlike markets, multiple independent instances of each facility configuration can be deployed to represent individual facilities.

Discrete Materials and Facilities

The Cyclus modeling infrastructure is designed such that every facility in a global nuclear fuel cycle is treated and acts individually. While modeling options exist to allow collective action, this will be as a special case of the individual facility basis. Each facility has two fundamental tasks: the transaction of goods or products with other facilities

and the transformation of those goods or products from an input form to an output form. For example, a reactor will receive fresh fuel assemblies from a fuel fabrication facility, transform them to used fuel assemblies using some approximation of the reactor physics, and supply those used fuel assemblies to a storage facility.

A facility configuration is created by selecting a FacilityModel and defining the parameters for that facility configuration. Each FacilityModel will define its own set of parameters that govern its performance. The same FacilityModel may be used for multiple facility configurations in the same region, each with parameter values appropriate for that facility configuration.

The repository model that is the subject of this work is a facility model within the Cyclus simulation paradigm.

Materials

Material movement is the primary unit of information in Cyclus . Materials passed, traded, and modified between and within facilities in the simulation are recorded at every timestep. This material history is stored in the output dataset of Cyclus . In addition to holding the map of isotopes and their masses, a material object holds a comprehensive history of its own path as it moves through models within the simulation.

Implications for Repository Model

The above sections outline the fuel cycle simulation platform currently under development at UW in which the repository model at hand is to be implemented. Implemented as a facility within this framework, the repository model interface is defined by the Facility Model interface defined within the Cyclus paradigm.

That interface requires that a capacity be defined by the repository at every Cyclus timestep so that the repository may make appropriate requests of disposable material.

Furthermore, the capability for dynamic module loading possible within the Cyclus paradigm allows the repository system subcomponents to be interchangeably loaded at runtime, enabling comparison of various repository subcomponents, physical models of varying levels of detail.

The repository is both a subclass and a superclass. It is a subclass of the FacilityModel class, and a superclass of its own subcomponents. That is, dynamically loaded subcomponents of the repository inherit data, parameters and behaviors from the repository itself.

2.2 Repository Modeling Paradigm

The repository model architecture is intended to modularly permit exchange of disposal system subcomponents, accept arbitrary spent fuel streams, and enable extending modules representing new or different component models.

Nested Component Concept

The fundamental unit of information in the repository model is the final nuclide release at the boundary of the far field resulting from nuclide release at each stage of containment. The repository model, in this way, is fundamentally a tool to determine the source term at the envrionmental surface as a result of an arbitrary waste stream. The repository model in this work conducts this calculation by treating each containment component as nested volumes in a release chain.

The capability to allow each component to define the components within it gives

this repository the ability to model many types of repository concept while maintaining a simple interface with the simulation.

Control Volumes

Each component of the repository system (i.e. waste form, waste package, buffer, and geologic medium) is modeled as a discrete control volume. Each control volume performs its own mass balance at each time step and assesses its own internal heat transfer and degradation phenomena separately from the other nested components.

Each control volume will initially be modeled as a mixed cell. That is, for permeable porous media, all contaminants released into the pore and fracture water are assumed to be uniformly distributed.

Thermal energy as well as mass will be conserved within each control volume by demanding continuity of thermal and mass fluxes accross the boundaries. Since radionuclide and thermal transport calculations internal to the control volumes may be represented by many models at varying levels of detail, abstraction on the component level against detailed models will be conducted to acheive appropriate detail in each component.

Information Passing Between Volumes

Each component passes some information radially outward to the nested component immediately containing it and some information radially inward to the nested component it contains. A diagram of the fundamental information being passed between components is described in Figure **??**.

Most component models require external information concerning the water volume that has breached containment, so information concerning incoming water volumes is

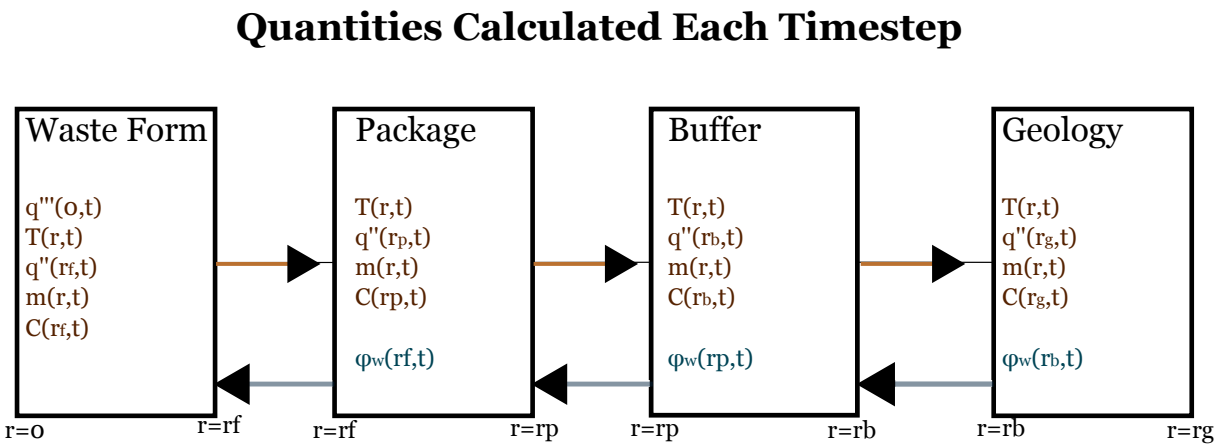

Figure 2.3: The nested components supply thermal flux and concentration information to each other at the boundaries.

passed radially inward.

Each component model similarly requires information about the radionuclides released from the component it immediately contains. Thus, nuclide release information is passed radially outward from the waste stream sequentially through each containment layer to the geosphere.

Components of the Nested System

The repository model is a collection of subcomponents which behave collectively to calculate repository metrics of interest. These subcomponents will be models of their own, and within the object oriented paradigm of the software will be a collection of module classes. Each component (i.e. waste form, waste package, buffer, lithology, etc.) will name a component superclass. Each superclass will be inherited by subclass models capable of representing that component in some level of detail specified by the model.

Waste Stream

The waste stream data object contains spent fuel isotopics over the course of the simulation. As radionuclides are gained, lost, and transmuted within the spent fuel object, a history of its isotopic composition is recorded.

For waste streams that vary from each other in composition, the thermal capacity of the repository must be recalculated. One way to model this will be to recalculate the appropriate lengthwise spacing of waste packages when the heat generation rate of a new package is significantly different than other waste packages in the repository.

Waste Form

The waste form model will calculate nuclide release due to dissolution of the waste form. Various heuristics by which nuclide release is modeled in accordance with waste form dissolution as well as the method by which the dissolution is modeled.

Dissolution can be instantaneous, rate based, water dependent, heat dependent, or coupled. Dissolution related release can be modeled as congruent, solubility limited, or both. Some radionuclides are immediately accessible, and some tend to remain in the fuel matrix.

Waste Package

The waste package model calculates nuclide release due to waste package failure. Waste package failure is typically modeled as instantaneous and complete or partial and constant. That is, a delay before full release, or a constantly present hole in the package.

Waste package time to failure is dependent on water contact and heat, but can be modeled as an average, probabilistic, or a rate.

In the case of highly deforming geologic media, such as salt, mechanical failure can be the primary mechanism for release from the waste package.

Buffer

Diffusion is the primary mechanism for nuclide transport through the buffer component of the repository system.

Salt, clay, and borehole repository concepts may not have a buffer material.

Backfill

Similarly, diffusion is the primary mechanism for nuclide transport through the buffer component of the repository system.

Clay concepts and borehole concepts may not have a backfill material.

Geological Environment

The literature review introduced various hydrological models that represent fluid and contaminant travel through permeable porous media and fractured porous media. These assume saturated flow and incorporate diffusive flow, advective flow, hydrodynamic dispersion, and equilibrium sorption. The geological environment control volume component will implement these models appropriately for each geologic environment to provide a mass balance and to communicate concentrations to adjacent components. Dirichlet boundary conditions at the surfaces of the control volume will allow the simulation to step through transport in the rock. Additional boundary condition types maybe implemented as extensions to the base case model.

Simulation Interface

The interface of the repository model with the Cyclus fuel cycle simulation interface is intended to be minimally restrictive, requiring only that the simulation supply waste stream information and provide a bookkeeping framework with which to record repository performance metrics. The repository model, in order to participate in the simulation as a facility model, must make requests for spent material up to its capacity. Determination of the repository capacity for various types of spent fuel commodities will comprise the interfacing functionality of the repository model. With the intention of developing the repository model in such a way as to be capable of interfacing with other simulation tools, however, calculation of metrics including expected dose rates and component failures will be the model's primary functionality.

Waste Stream Input

The repository model must accept arbitrary spent fuel and high level waste streams. Material objects resulting from the simulated fuel cycle arrive at the repository and are emplaced if all repository capacity limits allow it.

Since disposable material in most simulations of interest will be of variable composition and therefore heterogeneous in heat production capability, the repository model will repeatedly need to recalculate its own capacity as new materials are offered.

Repository Performance Metrics Calculated

Repository performance metrics that may be calculated from the source term and heat data calculated by the model will cover many metrics of interest to sustainability goals. Some metrics support analyses that seek to maximize safe repository capacity under

heat and source term limitations. Those include spatial dimensions, spatial dimensions per kWh or equivalent, repository footprint, and number of waste packages generated.

Still other metrics that may be calculated include those being considered by the UFD campaign in a Fuel Cycle Data Package task underway [**?**]. Additional metrics that will be considered in this context will likely include environmental metrics such as peak dose to the public, radiotoxic fluxes released to the biosphere integrated over time, and the minimum managed lifetime. These metrics are recorded in a database flexibly defined by the repository model.

Facility Functionality

The repository will behave as a facility within the Cyclus simulation paradigm. The fundamental facility behavior within Cyclus involves participating in commodity markets. The repository will participate as a requester of waste commodities. During reactor operation, the repository will make requests to markets dealing in spent fuel streams according to its available capacity. Possible optional intermediate storage facility model is available for cooling periods.

3 RADIONUCLIDE TRANSPORT SENSITIVITY ANALYSIS

The four GDSMss developed by the UFD campaign facilitate sensitivity analysis of the long-term post-closure performance of geologic repositories in generic media with respect to various key processes and parameters [**?**]. Processes and parameters expected to be influential to repository performance include the rate of waste form degradation, timing of waste package failure, and various coupled geochemical and hydrologic characteristics of the natural system including diffusion, solubility, and advection.

The results here provide an overview of the relative importance of processes that affect the repository performance of simplified generic disposal concepts. This work is not intended to give an assessment of the performance of a disposal system. Rather, it is intended to generically identify properties and parameters expected to influence repository performance in each geologic envrionment.

3.1 Approach

This analysis utilized four GDSMs developed by the UFD campaign to represent clay, granite, salt, and deep borehole repository concepts. Each GDSM performs detailed calculations of radionuclide transport within its respective geology [**?**].

The radionuclide transport calculations for the geologically distinct models are performed within the GoldSim simulation platform. GoldSim is a commercial simulation environment [**? ?**]. Probabilistic elements of the GoldSim modelling framework enable the models to incorporate simple probabilistic Features, Events, and Processes (FEPs) that affect repository performance including waste package failure, waste form dissolution, and an optional vertical advective fast pathway [**?**].

The GoldSim framework and its contaminant transport module provide a simula-

tion framework and radionuclide transport toolset that the GDSMs have utilized to simulate chemical and physical attenuation processes including radionuclide solubility, dispersion phenomena, and reversible sorption [**? ?**].

3.2 Mean of the Peak Annual Dose

In this analysis, repository performance is quantified by radiation dose to a hypothetical receptor. Specifically, this sensitivity analysis focuses on parameters that affect the mean of the peak annual dose. The mean of the peak annual dose,

$$D_{MoP,i} = \frac{\sum_{r=1}^{N} \max\left[D_{r,i}(t)|_{\forall t}\right]}{N} \tag{3.1}$$

where

$$\begin{aligned} D_{MoP,i} &= \text{mean of the peak annual dose due to isotope i}[mrem/yr] \\ D_i(t) &= \text{annual dose in realization r at time t due to isotope i } [mrem/yr] \\ N &= \text{Number of realizations,} \end{aligned}$$

is a conservative metric of repository performance. The mean of the peak annual dose should not be confused with the peak of the mean annual dose,

$$\begin{aligned} D_{PoM,i} &= \max\left[\frac{\sum_{r=1}^{N} D_{r,i}(t)|_{\forall t}}{N}\right] \\ &= \text{peak of the mean annual dose due to isotope i } [mrem/yr]. \end{aligned} \tag{3.2}$$

The mean of the peak annual dose rate given in equation (**??**) captures trends as well as the peak of the mean annual dose rate given in equation (**??**). However, the mean of the peaks metric, $D_{MoP,i}$, was chosen in this analysis because it is more conservative since it is able to capture temporally local dose maxima and consistently reports higher dose values than the peak of the means, $D_{PoM,i}$.

3.3 Sampling Scheme

The multiple barrier system modeled in the clay GDSM calls for a multi-faceted sensitivity analysis. The importance of any single component or environmental parameter must be analyzed in the context of the full system of barrier components and environmental parameters. Thus, this analysis has undertaken an analysis strategy to develop a many dimensional overview of the key factors in modeled repository performance.

To address this, both individual and dual parametric studies were performed. Individual parameter studies varied a single parameter of interest in detail over a broad range of values. Dual parameter sensitivity studies were performed for pairs of parameters expected to exhibit some covariance. For each parameter or pair of parameters, forty simulation groups varied the parameter or parameters within the range considered. Example tables of the resulting forty simulation groups for individual and dual parametric study configurations appear in Tables **??** and **??** respectively.

For each simulation group, a 100 realization simulation was completed. Each realization held the parameters being analyzed as constant and sampled stochastic values for uncertain parameters not being studied. A sampling scheme developed in previous generic disposal media modeling was implemented in this model in order to ensure that the each 100 realization simulation sampled identical values for uncertain parameters [**? ?**].

Individual Parameter Study

P	P_1	Group 1
	P_2	Group 2
	P_3	Group 3
	.	.
	.	.
	.	.
	P_{40}	Group 40

Table 3.1: For an individual one group of 100 realizations was run for each each discrete value, P_i, within the range considered for P.

Dual Parameter Study

		Q				
		Q_1	Q_2	Q_3	Q_4	Q_5
P	P_1	Group 1	Group 2	Group 3	Group 4	Group 5
	P_2	Group 6	Group 7	Group 8	Group 9	Group 10
	P_3	Group 11	Group 12	Group 13	Group 14	Group 15
	P_4	Group 16	Group 17	Group 18	Group 19	Group 20
	P_5	Group 21	Group 22	Group 23	Group 24	Group 25
	P_6	Group 26	Group 27	Group 28	Group 29	Group 30
	P_7	Group 31	Group 32	Group 33	Group 34	Group 35
	P_8	Group 36	Group 37	Group 38	Group 39	Group 40

Table 3.2: The simulation groups for a dual simulation sample each parameter within the range over which it was considered.

In order to independently analyze the dose contributions from radioisotope groups, four cases,

- Americium and its daughters,
- Plutonium and its daughters,
- Uranium and its daughters,
- Neptunium, its daughters, and fission products

were run independently. This allowed an evaluation of the importance of daughter production from distinct actinide chains.

3.4 Clay

These analyses were performed using the Clay GDSM developed by the UFD campaign[**?**]. The Clay GDSM is built on the GoldSim software and tracks the movement of key radionuclides through the natural system and engineered barriers [**? ?**].

The disposal concept modeled by the Clay GDSM includes an Engineered Barrier System (EBS) which can undergo rate based dissolution and barrier failure. Releases from the EBS enter near field and subsequently far field host rock regions in which diffusive and advective transport take place, attenuated by solubility limits as well as sorption and dispersion phenomena.

The Clay GDSM models a single waste form, a waste package, additional EBSs, an Excavation Disturbed Zone (EDZ), and a far field zone using a batch reactor mixing cell framework. This waste unit cell is modeled with boundary conditions such that it may be repeated assuming an infinite repository configuration. The waste form and engineered barrier system are modeled as well-mixed volumes and radial transport away from the cylindrical base case unit cell is modeled as one dimensional. Two radionuclide release pathways are considered. One is the nominal, undisturbed case, while the other is a fast pathway capable of simulating a hypothetical disturbed case [**?**].

Vertical Advective Velocity

Transport out of the EBS and through the permeable, porous geosphere involves advection, diffusion, and hydraulic dispersion phenomena. Advection is transport driven by bulk water velocity, while diffusion is the result of Brownian motion across concentration gradients. The method by which the dominant solute transport mode (diffusive or advective) is determined for a particular porous medium is by use of the dimensionless Peclet number,

$$
\begin{aligned}
Pe &= \frac{nvL}{\alpha nv + D_{eff}}, \\
&= \frac{\text{advective rate}}{\text{diffusive rate}}
\end{aligned}
\tag{3.3}
$$

where

$$
\begin{aligned}
n &= \text{ solute accessible porosity } [\%] \\
v &= \text{ advective velocity } [m \cdot s^{-1}] \\
L &= \text{ transport distance } [m] \\
\alpha &= \text{ dispersivity } [m] \\
D_{eff} &= \text{ effective diffusion coefficient } [m^2 \cdot s^{-1}].
\end{aligned}
$$

For a high Pe number, advection is the dominant transport mode, while diffusive or dispersive transport dominates for a low Pe number [**?**].

In this analysis, the threshold between primarily diffusive and primarily advective transport was investigated by varying the vertical advective velocity in conjunciton with the diffusion coefficient. It was expected that for the low diffusion coefficients and low advective velocities usually found in clay media, the model should behave entirely in the diffusive regime, but as the vertical advective velocity grows, system behavior should increasingly approach the advective regime.

Parametric Range

The diffusion coefficient was altered as in section **??** and the vertical advective velocity of the far field was altered as well.

From Table 5.5-1 of the Argile Safety Evaluation by ANDRA, the vertical hydraulic gradient is 0.4, while the hydraulic conductivity is $5.0 \times 10^{14}[m/s]$. The resulting vertical advective velocity is then $2.0 \times 10^{-14}[m/s]$, which is $6.31 \times 10^{-7}[m/yr]$ [**?**].

As in section **??**, in order to isolate the effect of the far field behavior, the waste form degradation rate was set to be very high as were the solubility and advective flow rate through the EBS. This guarunteed that in the first few time steps, the far field was the primary barrier to release.

The forty runs are a combination of the five values of the vertical advective velocity and eight magnitudes of relative diffusivity (see Table **??**).

		Vertical Advective Velocity [m/yr]				
		6.31E-08	6.31E-07	6.31E-06	6.31E-05	6.31E-04
		Groupings				
Reference Diffusivity (m^2/s)	1.E-08	1	2	3	4	5
	1.E-09	6	7	8	9	10
	1.E-10	11	12	13	14	15
	1.E-11	16	17	18	19	20
	1.E-12	21	22	23	24	25
	1.E-13	26	27	28	29	30
	1.E-14	31	32	33	34	35
	1.E-15	36	37	38	39	40

Table 3.3: Vertical advective velocity and diffusion coefficient simulation groupings.

To capture the importance of the vertical advective velocity, a range was chosen to span a number of orders of magnitude between 6.31×10^{-8} and $6.31 \times 10^{-4}[m/yr]$. The relative diffusivity was simultaneously varied over the eight magnitudes between 10^{-8} and $10^{-15}[m^2/s]$. It is worth noting that both the relative diffusivity and the vertical advective velocity are functions of porosity in the host rock and are therefore expected to vary together.

Results

For isotopes of interest, higher advective velocity and higher diffusivity lead to higher means of the peak annual dose. However, the relationship between diffusivity and advective velocity adds depth to the notion of a boundary between diffusive and advective regimes.

The highly soluble and non-sorbing elements, I and Cl were expected to exhibit behavior that is highly sensitive to advection in the system in the advective regime but less sensitive to advection in the diffusive regime.

In Figures **??**, **??**, **??**, and **??** , ^{129}I and ^{36}Cl are more sensitive to vertical advective velocity for lower vertical advective velocities. This demonstrates that for vertical advective velocities $6.31 \times 10^{-6}[m/yr]$ and above, lower reference diffusivities are ineffective at attenuating the mean of the peak doses for soluble, non-sorbing elements.

The solubility limited and sorbing elements, Tc and Np, in Figures **??**, **??**, **??**, and **??** show a very weak influence on peak annual dose rate for low reference diffusivities, but show a direct proportionality between dose and reference diffusivity above a threshold. For ^{99}Tc, for example, that threshold occurs at $1 \times 10^{-11}[m^2/s]$.

Dose contribution from ^{99}Tc has a proportional relationship with vertical advective velocity above a regime threshold at $6.31 \times 10^{-5}[m/yr]$, above which the system exhibits sensitivity to advection.

The convergence of the effect of the reference diffusivity and vertical advective velocity for the cases above shows the effect of dissolved concentration (solubility) limits and sorption. Se is non sorbing, but solubility limited. The results from ^{79}Se in Figure **??** and **??** show that for low vertical advective velocity, the system is diffusion dominated. However, for high vertical advective velocity, the diffusivity remains important even in the advective regime as spreading facilitates transport in the presence of solubility

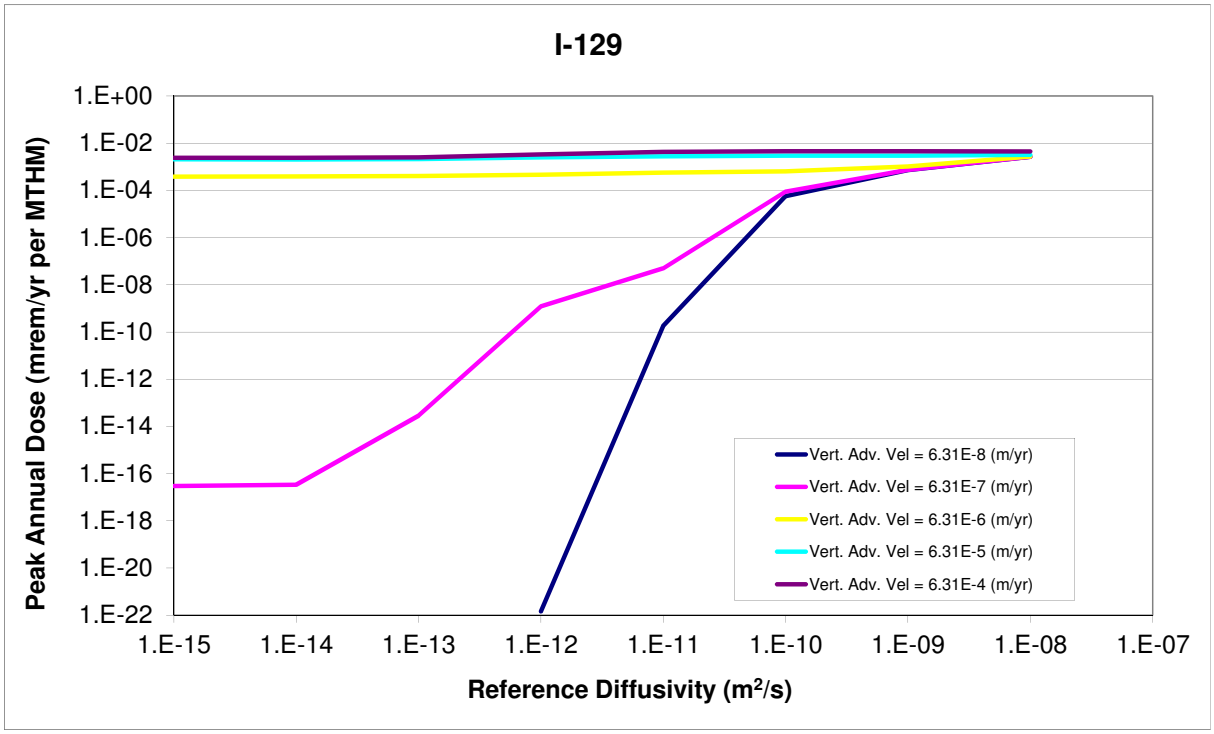

Figure 3.1: ^{129}I reference diffusivity sensitivity.

limited transport.

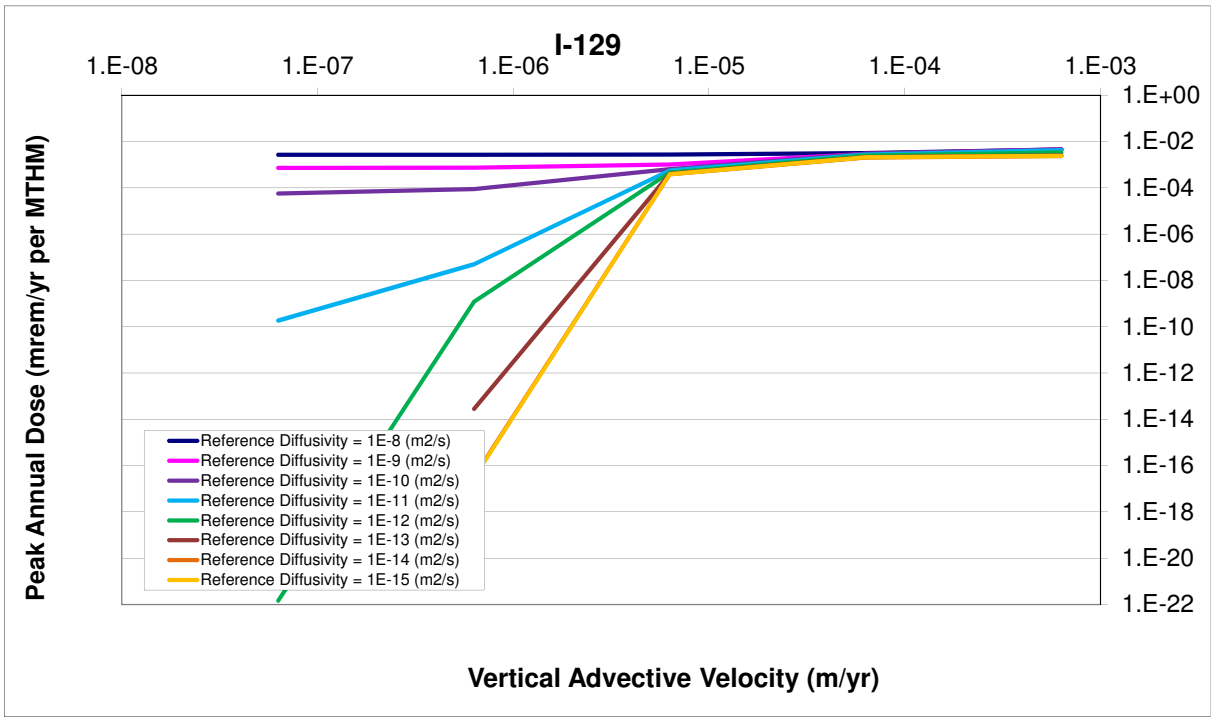

Figure 3.2: ^{129}I vertical advective velocity sensitivity.

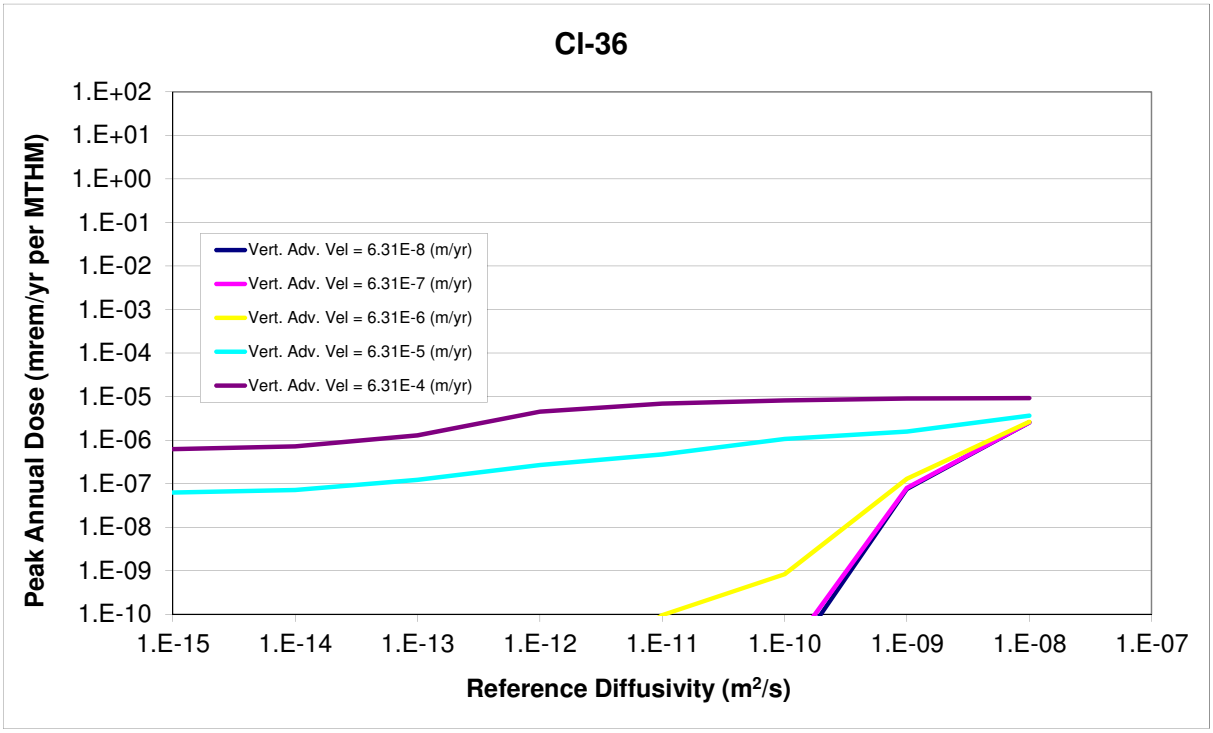

Figure 3.3: ^{36}Cl reference diffusivity sensitivity.

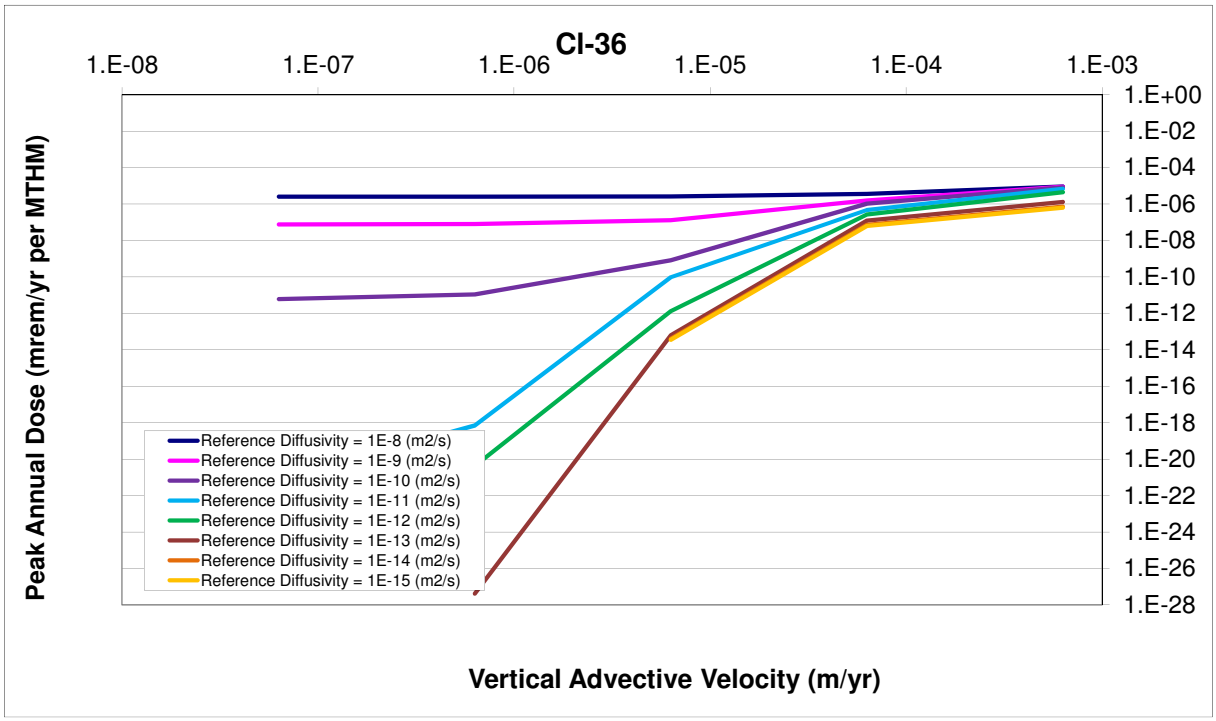

Figure 3.4: ^{36}Cl vertical advective velocity sensitivity.

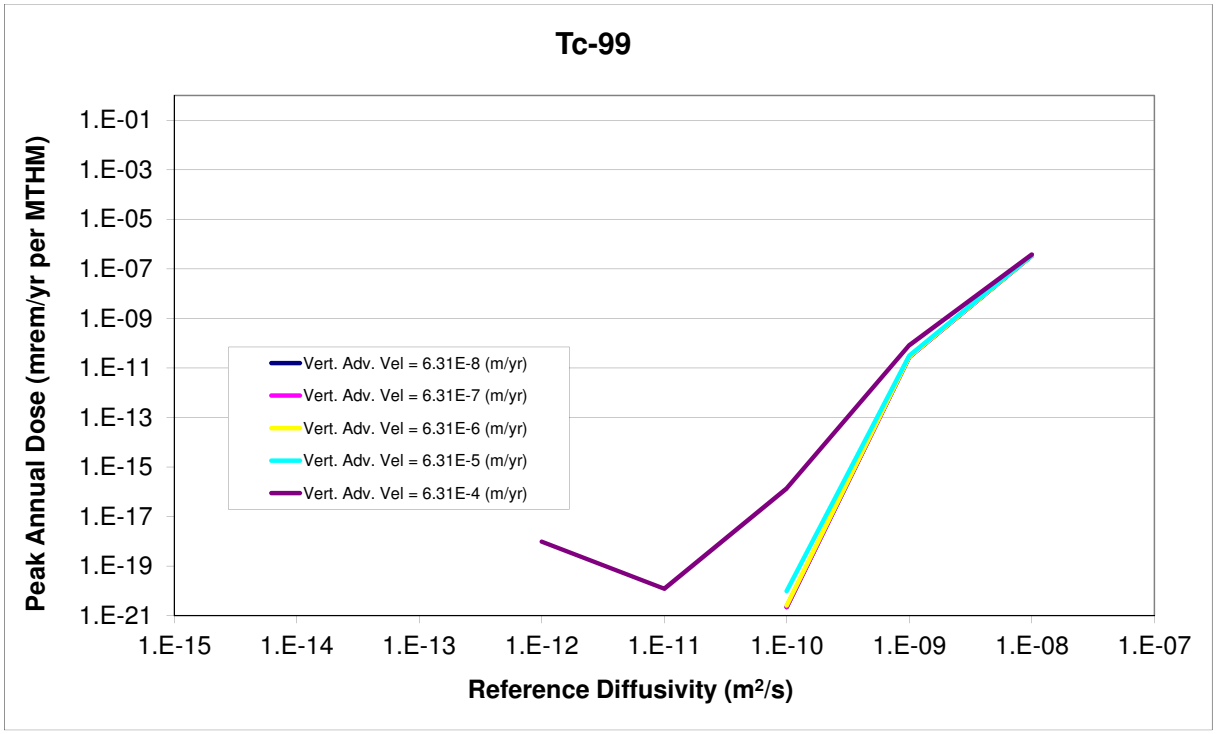

Figure 3.5: ^{99}Tc reference diffusivity sensitivity.

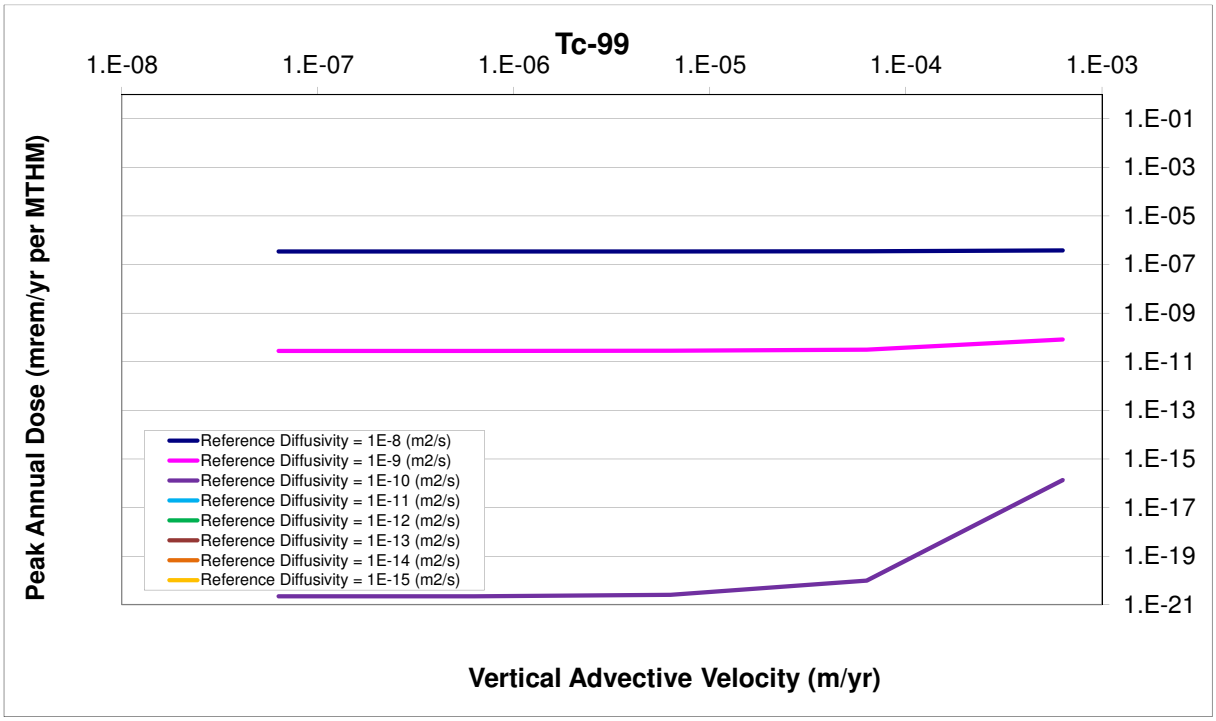

Figure 3.6: ^{99}Tc vertical advective velocity sensitivity.

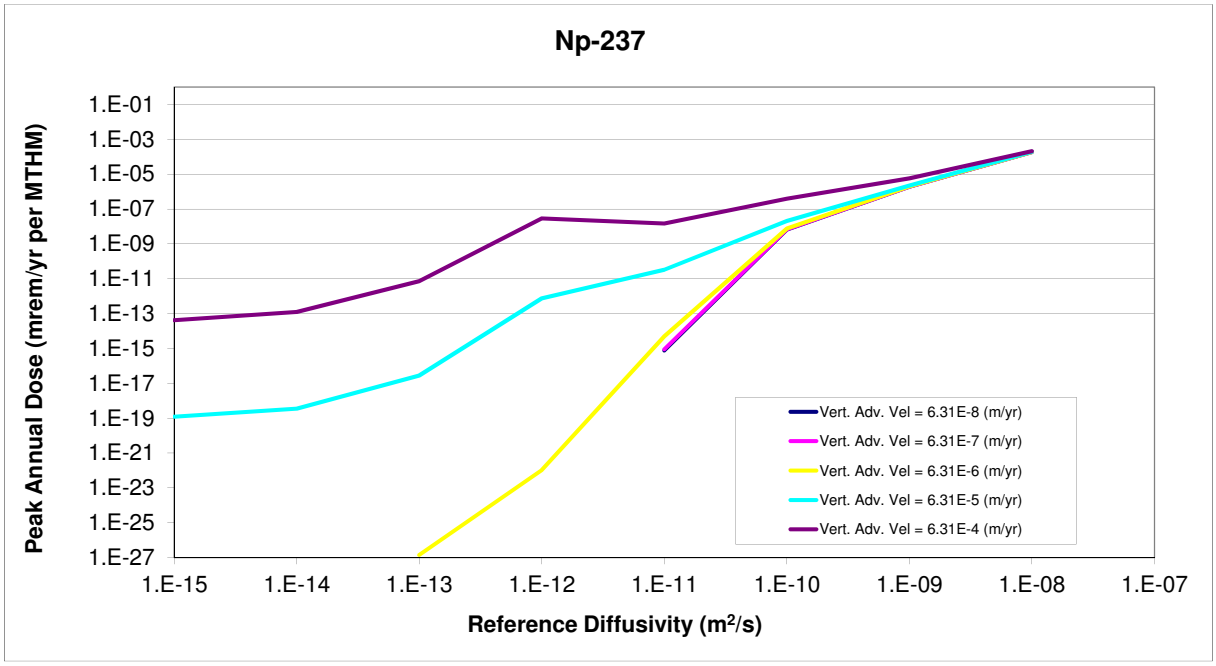

Figure 3.7: ^{237}Np reference diffusivity sensitivity.

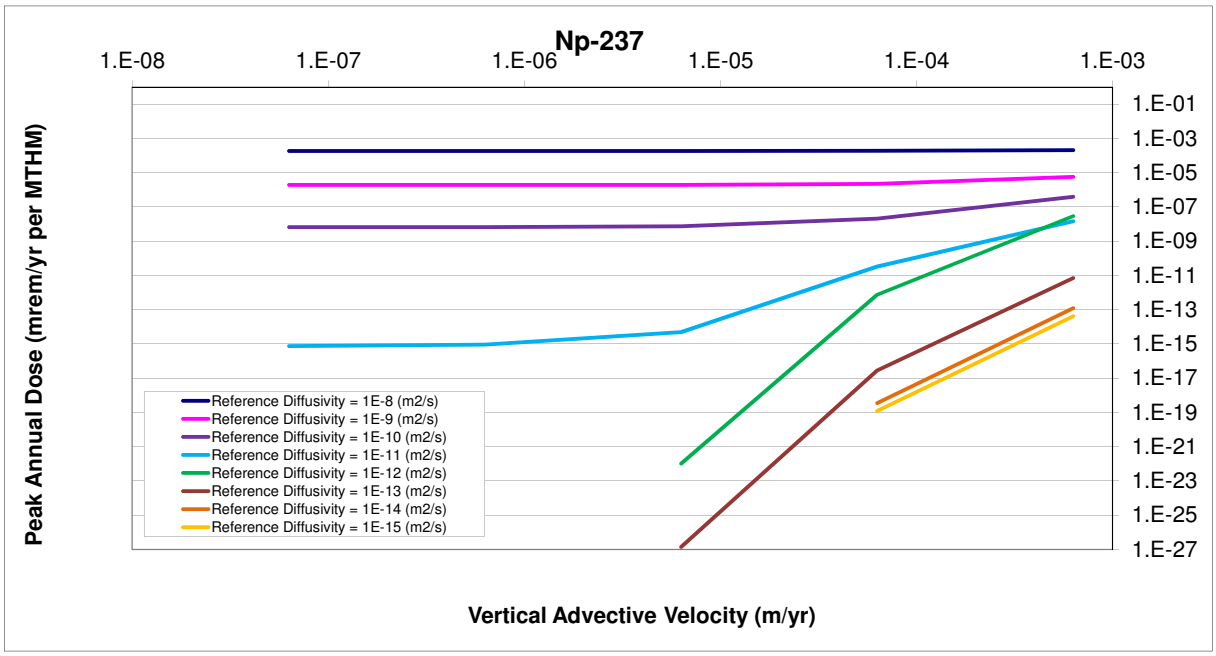

Figure 3.8: ^{237}Np vertical advective velocity sensitivity.

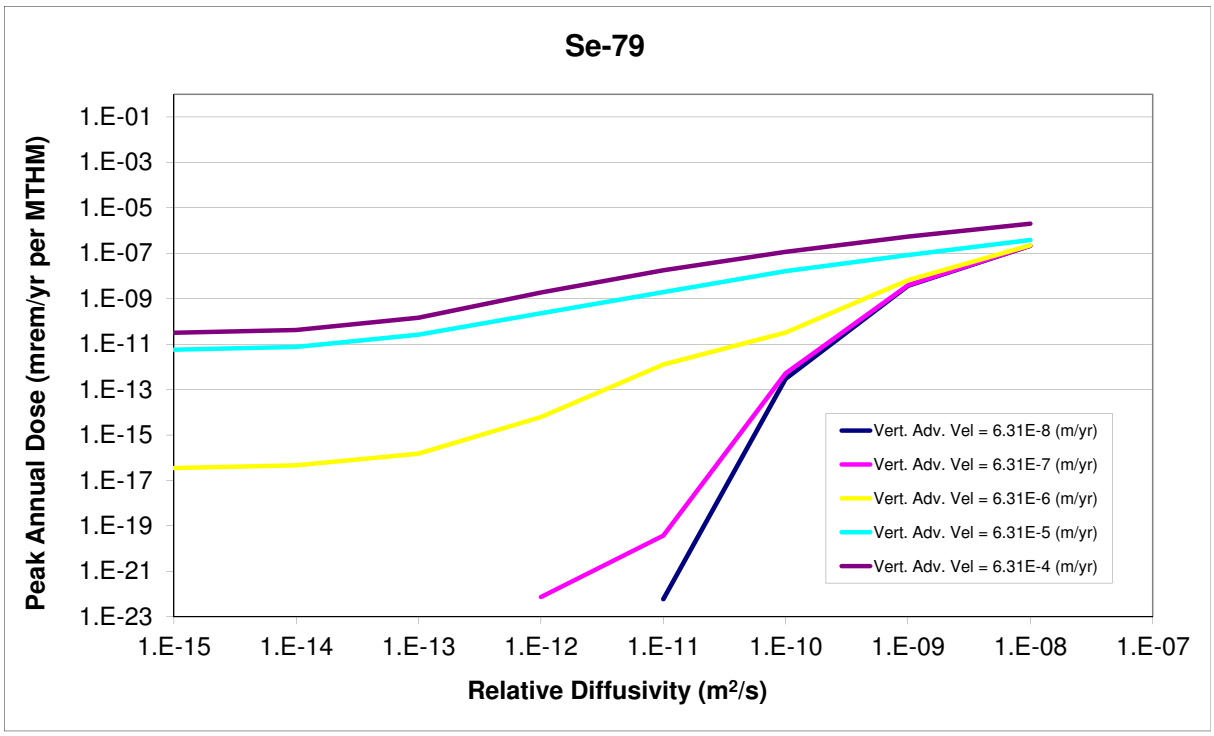

Figure 3.9: ^{79}Se reference diffusivity sensitivity.

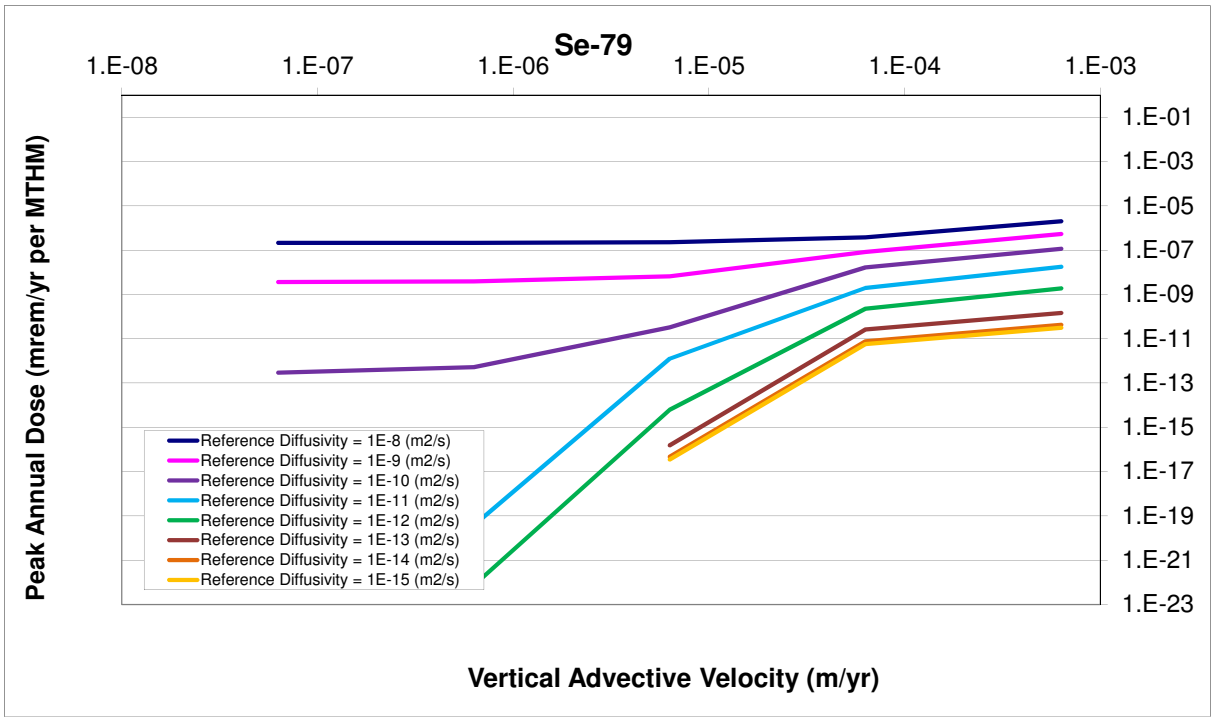

Figure 3.10: ^{79}Se vertical advective velocity sensitivity.

Diffusion Coefficient of Far Field

In clay media, diffusion dominates far field hydrogeologic transport due to characteristically low hydraulic head gradients and permeability. Thus, the effective diffusion coefficient is a parameter to which repository performance in clay media is expected to be very sensitive.

The sensitivity of the peak dose to the reference diffusivity of the host rock was analyzed. In this model, the reference diffusivity of the medium was the input parameter used to vary the effective diffusivity in a controlled manner. In GoldSim's transport module, the effective diffusion coefficient is defined as

$$D_{eff} = n\tau D_{ref} D_{rel} \tag{3.4}$$

$$\begin{aligned} D_{eff} &= \text{ effective diffusion coefficient } [m^2/s], \\ D_{rel} &= \text{ relative diffusivity for each isotope in water } [\%], \\ D_{ref} &= \text{ reference diffusivity in water } [m^2/s], \\ \tau &= \text{ tortuosity}[\%], \\ n &= \text{ porosity}[\%]. \end{aligned} \tag{3.5}$$

The reference diffusivity was altered while the porosity and the tortuosity were both set to 1. Thus, the simulation rendered the effective diffusivity equal to the product of the reference diffusivity and the relative diffusivity (set to 1 for all isotopes). This allowed the diffusivity to be controlled directly for all isotopes.

The waste inventory total mass was also altered for each value of the reference diffusivity. That is, the radionuclide inventory in a reference Metric Ton of Heavy Metal

(MTHM) of commercial spent nuclear fuel was multiplied by a scalar mass factor. It was expected that changing these two parameters in tandem would capture the importance of diffusivity in the far field to the repository performance as well as a threshold at which the effect of waste inventory dissolution is attenuated by solubility limits.

Finally, in order to isolate the effect of the far field behavior, the waste form degradation rate was set to be very high as were the solubility and advective flow rate through the EBS. This guaranteed that contaminant flowthrough in the near field was unhindered, leaving the far field as the dominant barrier to release.

Parametric Range

The forty runs corresponded to eight values of relative diffusivity and five values of inventory mass multiplier. That is, the reference diffusivity was varied over the eight magnitudes between 10^{-8} and 10^{-15} $[m^2/s]$. The Mass Factor, the unitless inventory multiplier, was simultaneously varied over the five magnitudes between 10^{-4} and $10^{1}[-]$. That is, the radionuclide inventory was varied between 10^{-4} and 10^{1} of that in one MTHM of SNF, which is expected to cover the full range of inventories in current wasteforms.

		Mass Factor				
		0.001	0.01	0.1	1	10
		Groupings				
Reference Diffusivity (m^2/s)	1.E-08	1	2	3	4	5
	1.E-09	6	7	8	9	10
	1.E-10	11	12	13	14	15
	1.E-11	16	17	18	19	20
	1.E-12	21	22	23	24	25
	1.E-13	26	27	28	29	30
	1.E-14	31	32	33	34	35
	1.E-15	36	37	38	39	40

Table 3.4: Diffusion coefficient and mass factor simulation groupings.

Results

The peak doses due to highly soluble, non-sorbing elements such as I and Cl, are proportional to the radionuclide inventory and largely directly proportional to the relative diffusivity. This can be seen for the cases of ^{129}I and ^{36}Cl in Figures **??**, **??**, **??** and **??**.

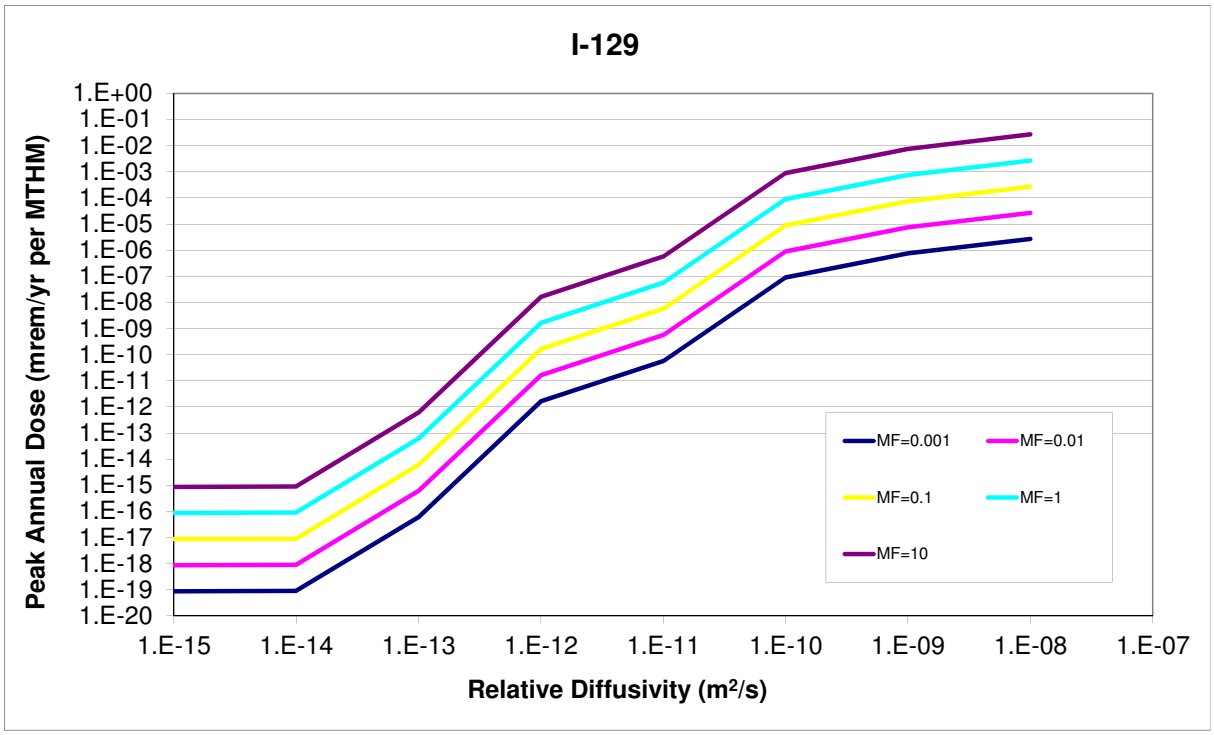

Figure 3.11: ^{129}I relative diffusivity sensitivity.

Long lived ^{129}I and ^{36}Cl are assumed to have near complete solubility, so in Figures **??** and **??**, the effect of a solubility limited attenuation regime is not seen. Even for very low diffusivities, the diffusion length of the far field is the primary barrier. In Figures **??** and **??** it is clear that in the absence of solubility limitation and sorption, the peak dose is directly proportional to mass factor.

Both Cl and I are soluble and non-sorbing. The amount of ^{129}I in the SNF inventory

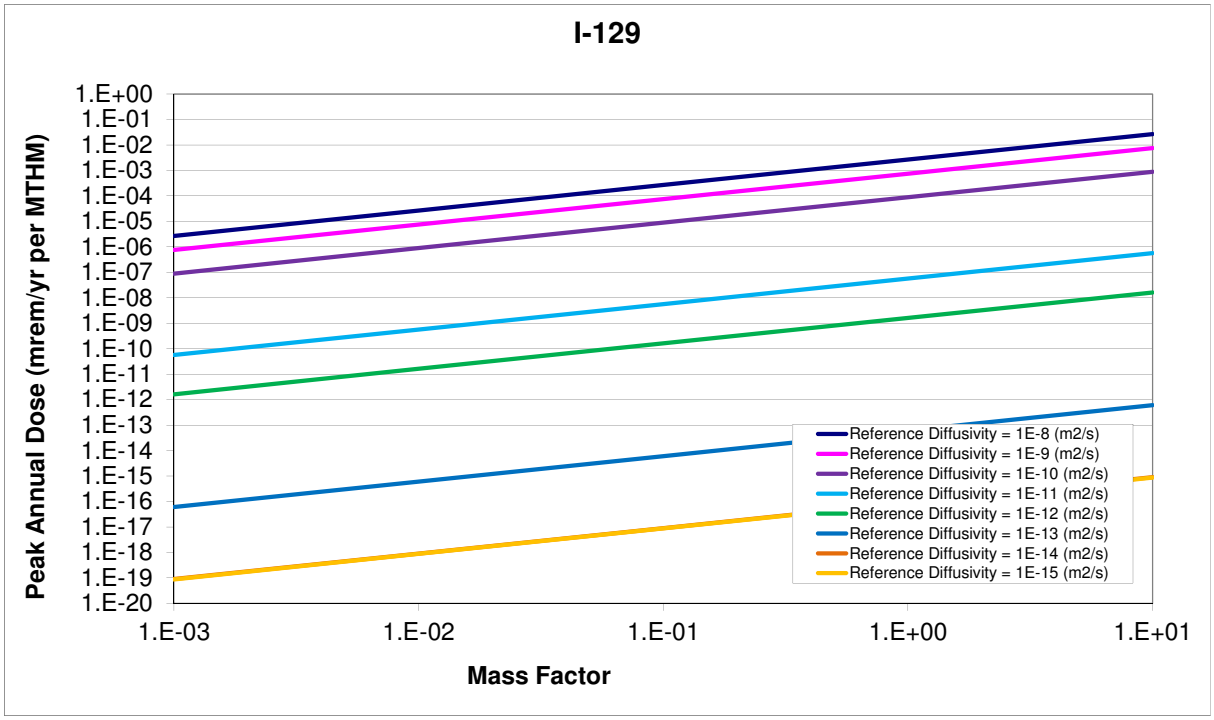

Figure 3.12: ^{129}I mass factor sensitivity.

is greater than the amount of ^{36}Cl, so a difference in magnitudes are expected, however, the trends should be the same. Since the halflife of ^{36}Cl, $3 \times 10^5[yr]$, is much shorter than the half life of ^{129}I, $1.6 \times 10^7[yr]$, a stronger proportional dependence on mass factor is seen for Cl due to its higher decay rate.

With the exception of those dose-contributors assumed to be completely soluble, two regimes were visible in the results of this analysis. In low diffusion coefficient regime, the diffusive pathway through the homogeneous permeable porous medium in the far field continues to be a dominant barrier to nuclide release for normal (non-intrusive) repository conditions.

In the second regime, for very high diffusion coefficients, the effects of additional attenuation phenomena in the natural system can be seen. The dependence of peak annual dose on mass factor was consistently directly proportional for all isotopic groups.

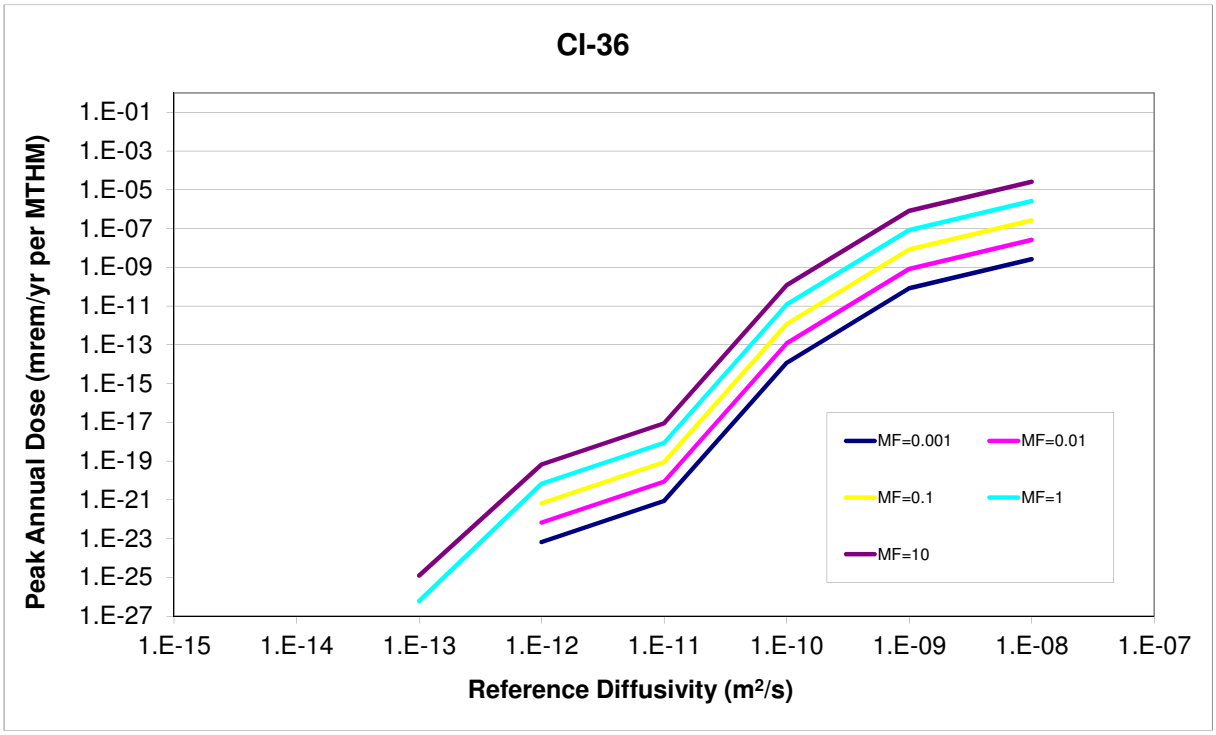

Figure 3.13: ^{36}Cl relative diffusivity sensitivity.

The peak doses due to solubility limited, sorbing elements such as Np and Tc demonstrate two major regimes. In the first regime, for low values of mass factor, the mean of the peak annual dose rates is directly proportional to both reference diffusivity and mass factor. For higher values of mass factor, the sensitivity to reference diffusivity and mass factor are both attenuated at higher values. The attenuation in these regimes is due to natural system attenuation, most notably, sorption.

^{237}Np and ^{99}Tc exhibit a strong proportional relationship between diffusivity and dose in Figures **??** and **??**. This relationship is muted as diffusivity increases. Both are directly proportional to mass factor until they reach the point of attenuation by their solubility limits, as can be seen in Figures **??** and **??**.

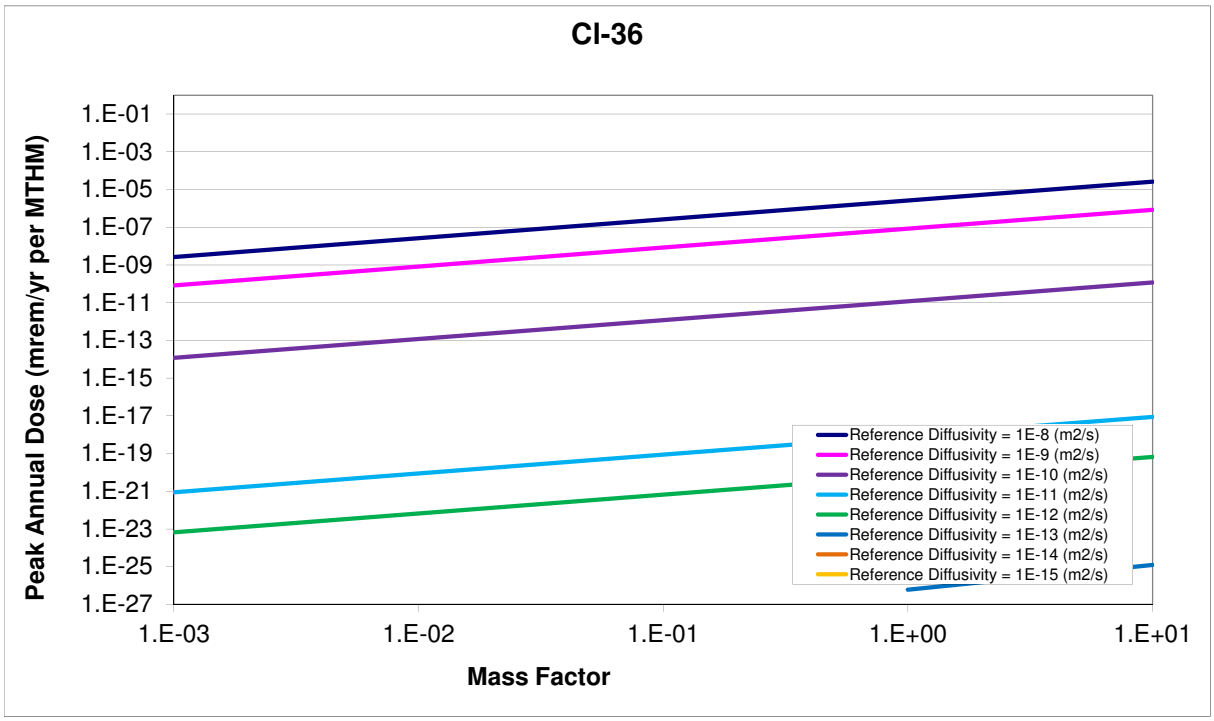

Figure 3.14: ^{36}Cl mass factor sensitivity.

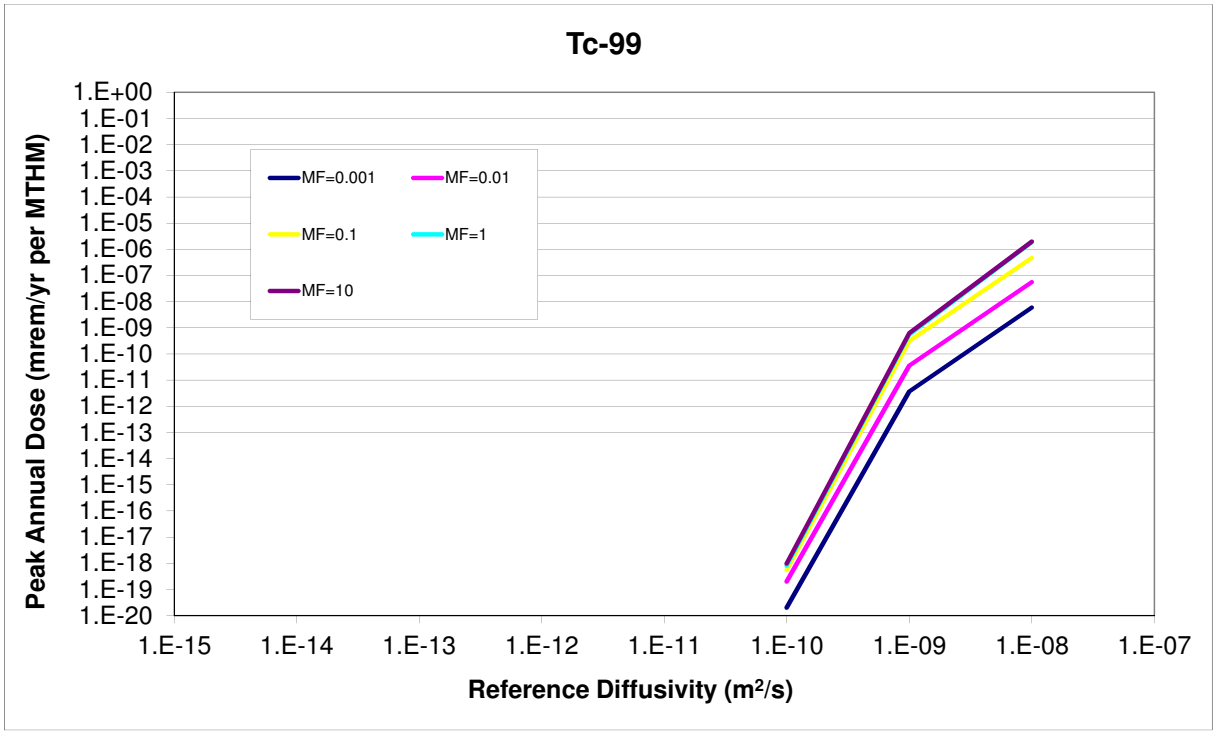

Figure 3.15: ^{99}Tc relative diffusivity sensitivity.

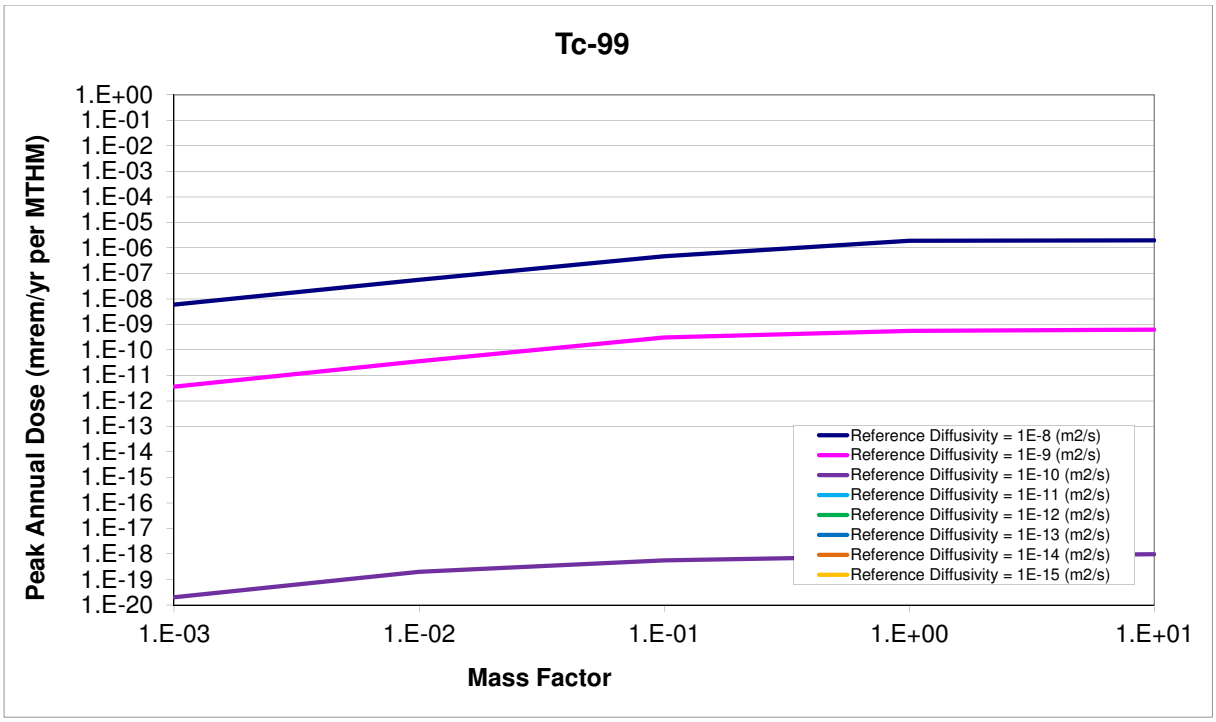

Figure 3.16: ^{99}Tc mass factor sensitivity.

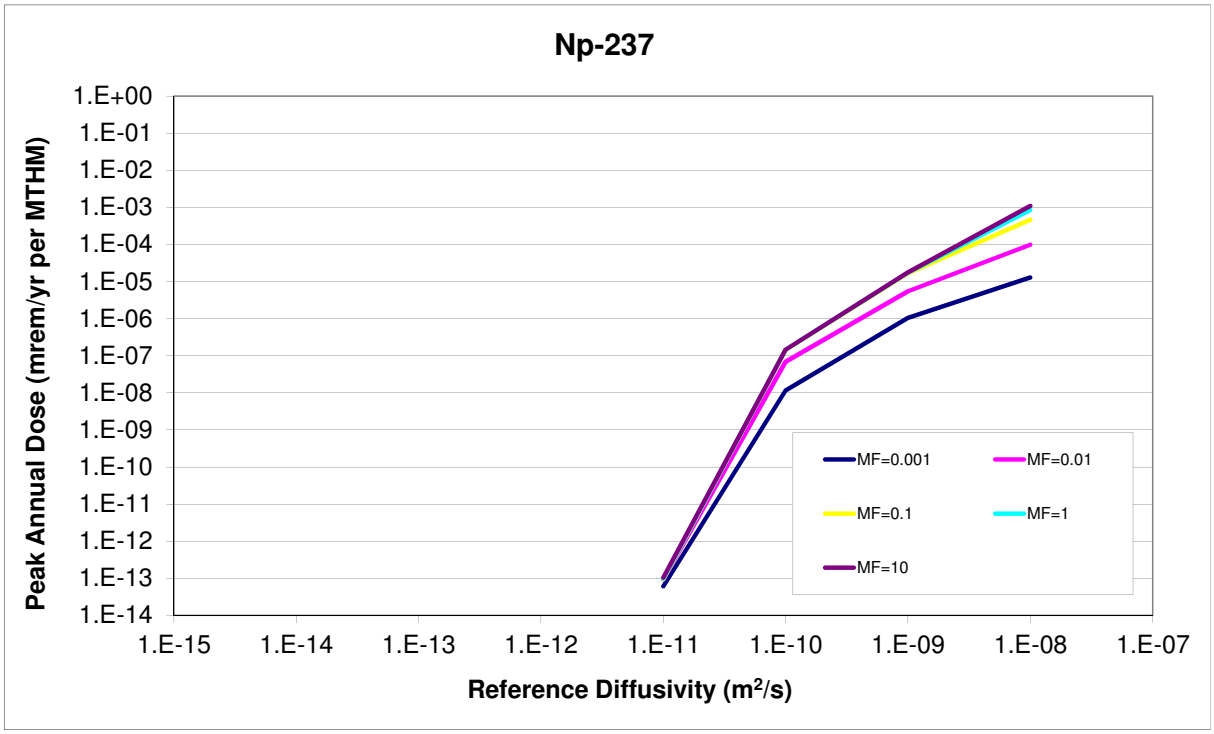

Figure 3.17: ^{237}Np relative diffusivity sensitivity.

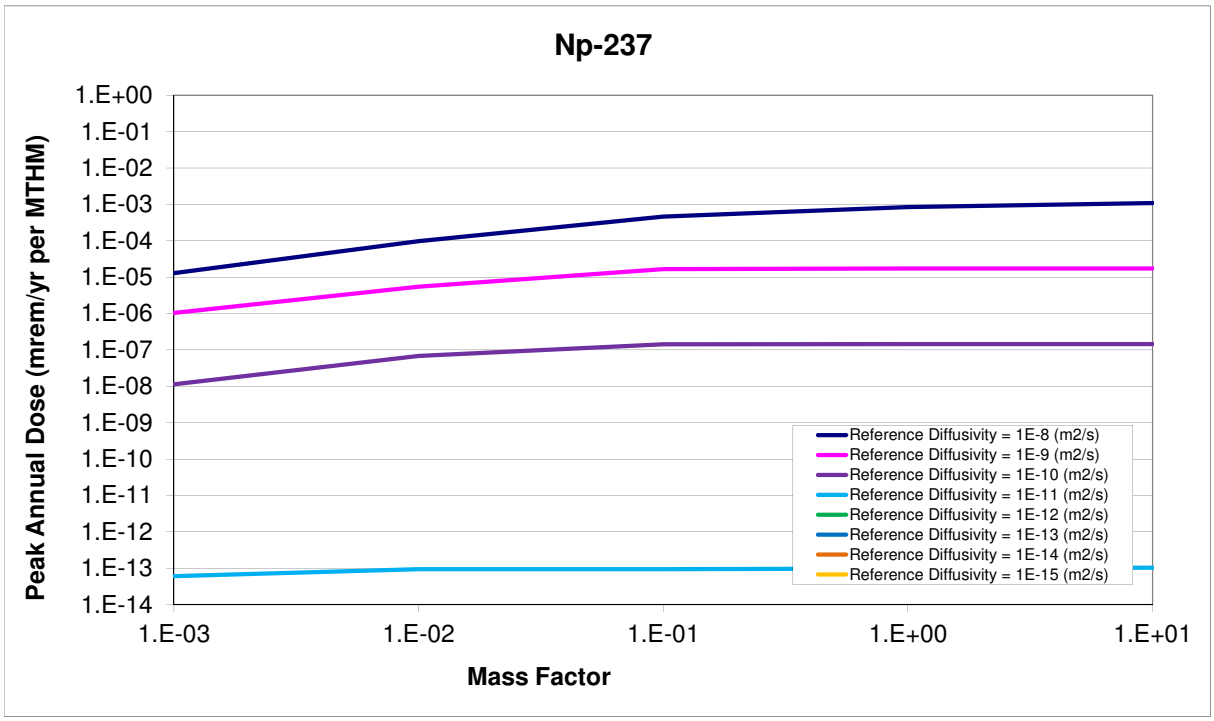

Figure 3.18: ^{237}Np mass factor sensitivity.

Solubility Coefficients

This study varied the solubility coefficients for each isotope in the simulation to help inform the effect of reprocessing on repository benefit for the clay repository scenario. The importance of the actinide contribution relative to the contribution from ^{129}I, ^{79}Se, and ^{99}Tc was of particular interest.

The dissolution behavior of a solute in an aqueous solutions is called its solubility. This behavior is limited by the solute's solubility limit, described by an equilibrium constant that depends upon temperature, water chemistry, and the properties of the element. The solubility constant for ordinary solutes, K_s gives units of concentration, $[kg/m^3]$, and can be determined algebraically by the law of mass action which gives the partitioning at equilibrium between reactants and products. For a reaction

$$cC + dD = yY + zZ, \tag{3.6}$$

where

$$\begin{aligned} c, d, y, z &= \text{ amount of respective constituent } [mol] \\ C, D &= \text{ reactants } [-] \\ Y, Z &= \text{ products } [-], \end{aligned}$$

the law of mass action gives

$$K = \frac{(Y)^y (Z)^z}{(C)^c (D)^d} \tag{3.7}$$

where

$$(X) = \text{ the equilibrium molal concentration of X } [mol/m^3]$$
$$K = \text{ the equilibrium constant } [-].$$

The equilibrium constant for many reactions are known, and can be found in chemical tables. Thereafter, the solubility constraints of a solution at equilibrium can be found algebraically. In cases of salts that dissociate in aqueous solutions, this equilibrium constant is called the salt's solubility product K_{sp}.

This equilibrium model, however, is only appropriate for dilute situations, and nondilute solutions at partial equilibrium must be treated with an activity model by substituting the activities of the constituents for their molal concentrations,

$$[X] = \gamma_x(X) \tag{3.8}$$

where

$$[X] = \text{ activity of X } [-]$$
$$\gamma_x = \text{ activity coefficient of X}[-]$$
$$(X) = \text{ molal concentration of X}[mol/m^3]$$

such that

$$IAP = \text{ Ion Activity Product } [-].$$
$$= \frac{[Y]^y[Z]^z}{[C]^c[D]^d} \tag{3.9}$$
$$\tag{3.10}$$

The ratio between the IAP and the equilibrium constant (IAP/K) quantifiesn the departure from equilibrium of a solution. This information is useful during the transient stage in which a solute is first introduced to a solution. When $IAP/K < 1$, the solution is undersaturated with respect to the products. When, conversely, $IAP/K > 1$, the solution is oversaturated and precipitation of solids in the volume will occur.

Parametric Range

The solubility coefficients were varied in this simulation using a multiplier. The reference solubilities for each element were multiplied by the multiplier for each simulation group. This technique preserved relative solubility among elements. Forty values of solubility coefficient multiplier were used to change the far field solubility. This did not alter any of the solubility in the EDZ, WF, or Fast Path solubilities.

The values of the solubility multiplier were deliberately varied over many magnitudes, from 1^{-9} through 5×10^{10}. This multiplier multiplied the most likely values of solubility for each element, so the relative solubility between elements was preserved.

Results

The results for varying the solubility coefficient were very straightforward. For solubility limits below a certain threshold, the dose releases were directly proportional to the

solubility limit, indicating that the radionuclide concentration saturated the groundwater up to the solubility limit near the waste form. For solubility limits above the threshold, however, further increase to the limit had no effect on the peak dose. This demonstrates the situation in which the solubility limit is so high that even complete dissolution of the waste inventory into the pore water is insufficient to reach the solubility limit.

In Figures **??** and **??**, it is clear that for solubility constants lower than a threshold, the relationship between peak annual dose and solubility limit is strong.

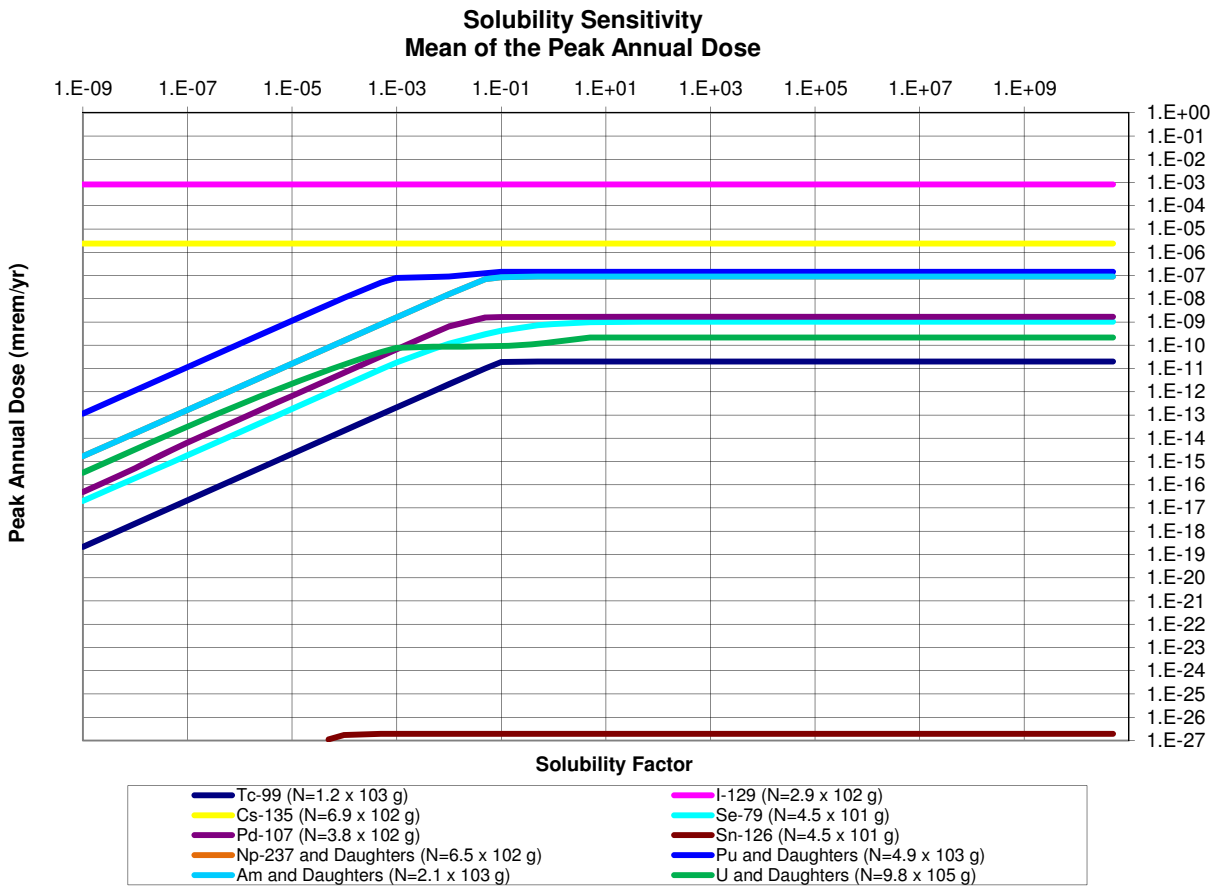

Figure 3.19: Solubility factor sensitivity. The peak annual dose due to an inventory, N, of each isotope.

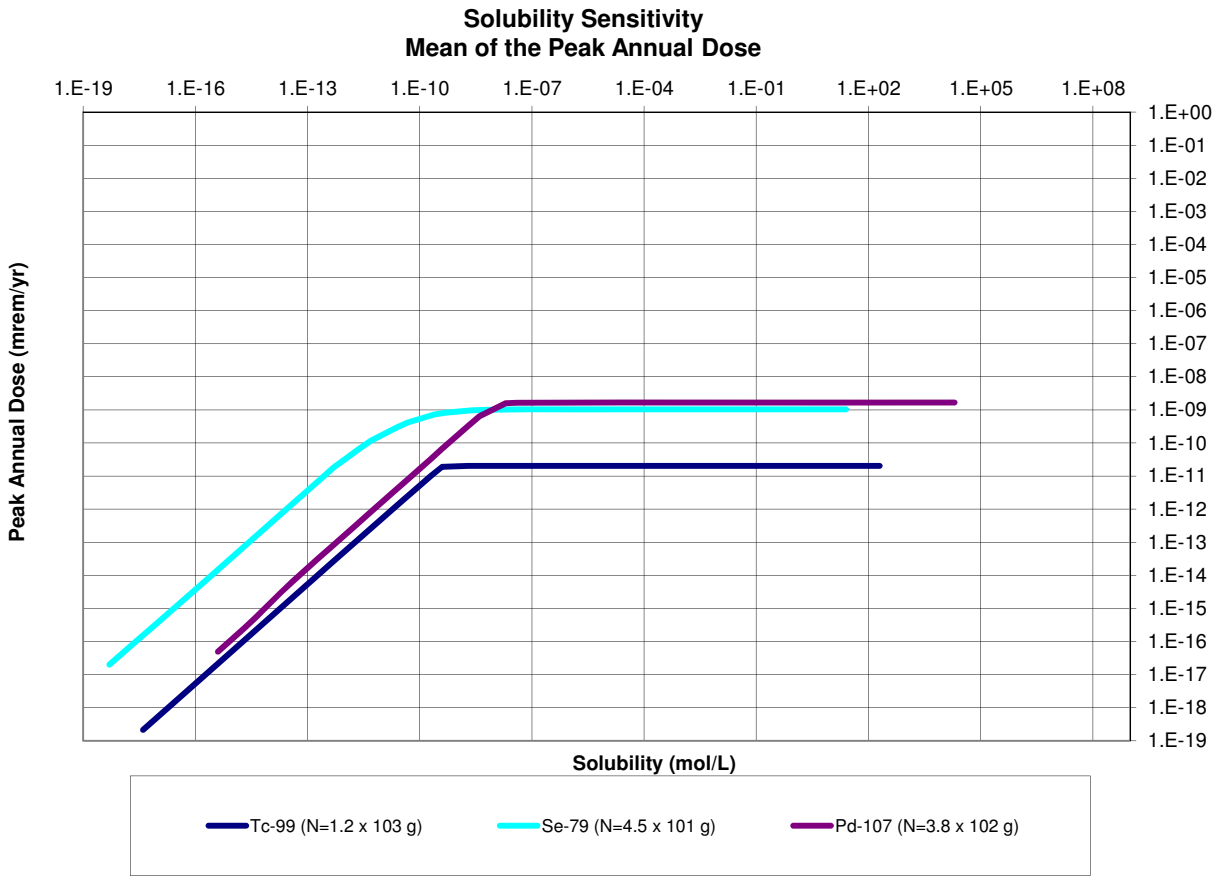

Figure 3.20: Solubility limit sensitivity. The peak annual dose due to an inventory, N, of each isotope.

The Partition Coefficient

This analysis investigated the peak dose rate contribution from various radionuclides to the partition coefficient of those radionuclides.

The partition or distribution coefficient, K_d, relates the amount of contaminant adsorbed into the solid phase of the host medium to the amount of contaminant adsorbed into the aqueous phase of the host medium. It is a common empirical coefficient used to capture the effects of a number of retardation mechanisms. The coefficient K_d, in units of $[m^3 \cdot kg^{-1}]$, is the ratio of the mass of contaminant in the solid to the mass of contaminant in the solution.

The retardation factor, R_f, which is the ratio between velocity of water through a volume and the velocity of a contaminant through that volume, can be expressed in terms of the partition coefficient,

$$R_f = 1 + \frac{\rho_b}{n_e} K_d \tag{3.11}$$

where

$$\rho_b = \text{ bulk density}[kg \cdot m^{-3}]$$

and

$$n_e = \text{ effective porosity of the medium}[\%].$$

Parametric Range

The parameters in this model were all set to the default values except a multiplier applied to the partitioning K_d coefficients.

The multiplier took the forty values $1 \times 10^{-9}, 5 \times 10^{-8}, \cdots 5 \times 10^{10}$ Only the far field partition coefficients were altered by this factor. Partition coefficients effecting the EDZ and fast pathway were not changed.

Results

The expected inverse relationship between the retardation factor and resulting peak annual dose was found for all elements that were not assumed to be effectively infinitely soluble. In the low retardation coefficient cases, a regime is established in which the peak annual dose is entirely unaffected by changes in retardation coefficient. For large values of retardation coefficient, the sensitivity to small changes in the retardation coefficient increases dramatically. In that sensitive regime, the change in peak annual dose is inversely related to the retardation coefficient. Between these two regimes was a transition regime, in which the K_d factor ranges from 1×10^{-5} to $5 \times 10^{0}[-]$.

It is clear from Figures **??** and **??** that for retardation coefficients greater than a threshold, the relationship between peak annual dose and retardation coefficient is a strong inverse one.

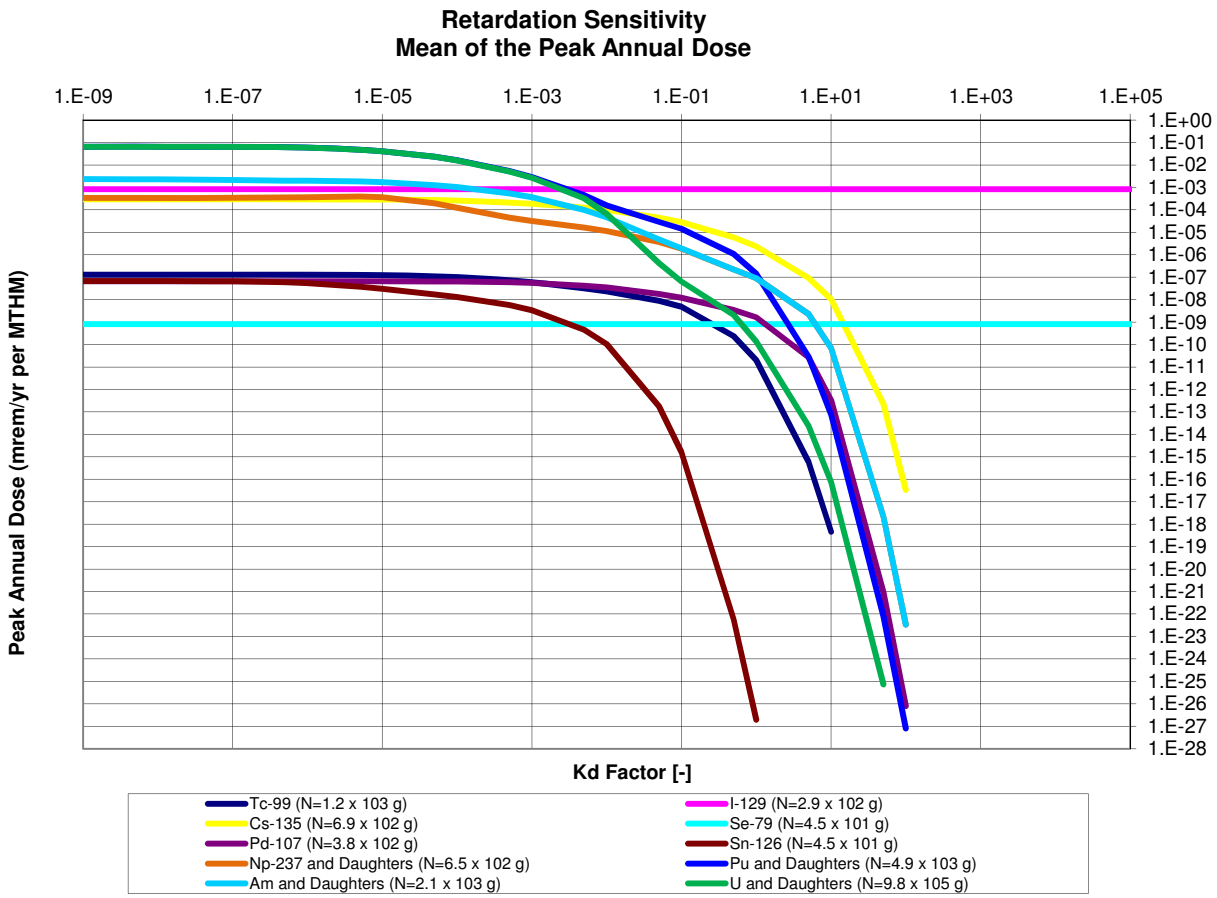

Figure 3.21: K_d factor sensitivity. The peak annual dose due to an inventory, N, of each isotope.

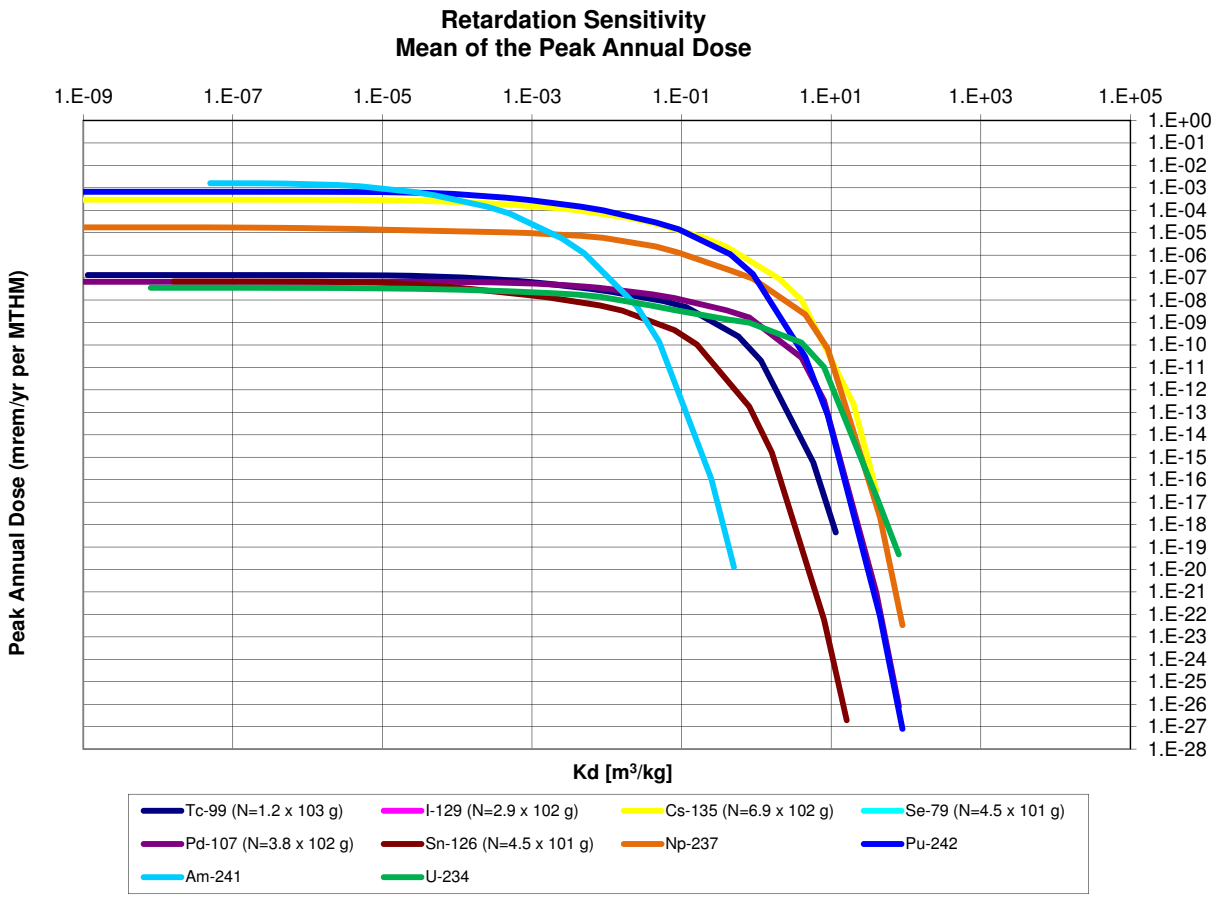

Figure 3.22: K_d sensitivity. The peak annual dose due to an inventory, N, of each isotope.

Waste Form Degradation Rate

The sensitivity of peak dose rate to the waste form degradation rate was determined with respect to varying inventories of waste.

The sensitivity of repository performance to waste form degradation rate was expected to vary according to the waste inventory. For cases in which the dominant dose contributing radionuclides have half-lives much shorter than the expected waste form lifetime, the waste form degradation rate is not expected to have an effect. So too, for cases in which the primary barrier to release, the slow diffusive pathway, dominates overall repository performance, the waste form engineered barrier was expected to have a negligible effect on repository performance in comparison.

In the case of a clay repository, the effect of the long time scale of the diffusive release pathway was to dampen the potential effect of high waste form degradation rates.

Parametric Range

These runs varied the waste form degradation rate and the waste inventory mass factor. There were forty runs corresponding to eight values of the waste form degradation rate and five values of the mass factor.

The waste form degradation rate was varied over the eight magnitudes between 10^{-9} and $10^{-2}[1/yr]$. The inventory mass factor was varied over the five magnitudes between 0.001 and $10.0[-]$.

Results

These results show two regimes. In the first regime, the mean of the peak annual dose rates is directly proportional to both the mass factor and the fractional waste form degradation rate. For some radionuclides, attenuation occurs for high values of both

parameters as the release of radionuclides is limited by dispersion parameters. This phenomenon can be seen in the figures below in which transition between regimes for higher degradation rates happens at lower mass factors than transition between regimes for lower degradation rates.

Safety indicators for post closure repository performance have been developed by the UFD campaign which utilize the inventory multiplier that was varied in this study [**?**]. These indicators are normalized by a normalization factor (100 mrem/yr) recommended by the International Atomic Energy Agency (IAEA) as the limit to "relevant critical members of the public" [**?**]. The functional form for this safety indicator for a single waste category, high level waste (HLW), is just

$$SI_G = \left(\frac{\sum_{i=1}^{N} D_{G,i}(I_i, F_d)}{100mrem/yr} \right) [GWe/yr]. \tag{3.12}$$

where

$$\begin{aligned} SI_G &= \text{Safety indicator for disposal in media type G}[GWe/yr] \\ N &= \text{Number of key radionuclides considered in this indicator} \\ D_{G,i} &= \text{Peak dose rate from isotope i in media type G}[mrem/yr] \\ F_d &= \text{Fractional waste form degradation rate}[1/yr]. \end{aligned}$$

Tables **??**, **??**, and **??** report the safety indicators for various independent isotopes and, where applicable, their daughters.

		Inventory Factor				
		0.001	0.01	0.1	1	10
		I-129 (N=2.9 x 10^2 g)				
Degradation Rate	1.E-09	3.E-11	3.E-10	3.E-09	3.E-08	3.E-07
	1.E-08	3.E-10	3.E-09	3.E-08	3.E-07	3.E-06
	1.E-07	2.E-09	2.E-08	2.E-07	2.E-06	2.E-05
	1.E-06	8.E-09	8.E-08	8.E-07	8.E-06	8.E-05
	1.E-05	1.E-08	1.E-07	1.E-06	1.E-05	1.E-04
	1.E-04	1.E-08	1.E-07	1.E-06	1.E-05	1.E-04
	1.E-03	1.E-08	1.E-07	1.E-06	1.E-05	1.E-04
	1.E-02	1.E-08	1.E-07	1.E-06	1.E-05	1.E-04
		Cl-36 (N=1 g)				
Degradation Rate	1.E-09	1.E-15	1.E-14	1.E-13	1.E-12	1.E-11
	1.E-08	1.E-14	1.E-13	1.E-12	1.E-11	1.E-10
	1.E-07	1.E-13	1.E-12	1.E-11	1.E-10	1.E-09
	1.E-06	9.E-13	9.E-12	9.E-11	9.E-10	9.E-09
	1.E-05	3.E-12	3.E-11	3.E-10	3.E-09	3.E-08
	1.E-04	4.E-12	4.E-11	4.E-10	4.E-09	4.E-08
	1.E-03	4.E-12	4.E-11	4.E-10	4.E-09	4.E-08
	1.E-02	4.E-12	4.E-11	4.E-10	4.E-09	4.E-08

Table 3.5: Safety indicators for soluble, non-sorbing nuclides.

		Inventory Factor				
		0.001	0.01	0.1	1	10
		Pd-107 (N=3.8 x 10^2 g)				
Degradation Rate	1.E-09	2.E-16	2.E-15	2.E-14	2.E-13	2.E-12
	1.E-08	2.E-15	2.E-14	2.E-13	2.E-12	1.E-11
	1.E-07	2.E-14	2.E-13	2.E-12	8.E-12	3.E-11
	1.E-06	5.E-14	5.E-13	3.E-12	2.E-11	3.E-11
	1.E-05	5.E-14	5.E-13	4.E-12	2.E-11	3.E-11
	1.E-04	5.E-14	5.E-13	4.E-12	2.E-11	3.E-11
	1.E-03	5.E-14	5.E-13	4.E-12	2.E-11	3.E-11
	1.E-02	5.E-14	5.E-13	4.E-12	2.E-11	3.E-11
		Sn-126 (N=4.5 x 10^1 g)				
Degradation Rate	1.E-09	0.E+00	0.E+00	0.E+00	0.E+00	0.E+00
	1.E-08	0.E+00	0.E+00	0.E+00	0.E+00	0.E+00
	1.E-07	0.E+00	0.E+00	0.E+00	0.E+00	2.E-29
	1.E-06	0.E+00	0.E+00	0.E+00	2.E-29	5.E-29
	1.E-05	0.E+00	0.E+00	1.E-29	3.E-29	5.E-29
	1.E-04	0.E+00	0.E+00	1.E-29	3.E-29	5.E-29
	1.E-03	0.E+00	0.E+00	1.E-29	3.E-29	5.E-29
	1.E-02	0.E+00	0.E+00	1.E-29	3.E-29	5.E-29
		Zr-93 & Nb-93				
Degradation Rate	1.E-09	1.E-17	1.E-16	1.E-15	1.E-14	1.E-13
	1.E-08	1.E-16	1.E-15	1.E-14	1.E-13	7.E-13
	1.E-07	1.E-15	1.E-14	1.E-13	6.E-13	3.E-12
	1.E-06	4.E-15	4.E-14	3.E-13	1.E-12	4.E-12
	1.E-05	6.E-15	6.E-14	4.E-13	2.E-12	4.E-12
	1.E-04	6.E-15	6.E-14	4.E-13	2.E-12	4.E-12
	1.E-03	7.E-15	6.E-14	4.E-13	2.E-12	4.E-12
	1.E-02	7.E-15	6.E-14	4.E-13	2.E-12	4.E-12
		Tc-99 (N=1.2 x 10^3 g)				
Degradation Rate	1.E-09	2.E-18	2.E-17	2.E-16	2.E-15	2.E-14
	1.E-08	2.E-17	2.E-16	2.E-15	2.E-14	1.E-13
	1.E-07	2.E-16	2.E-15	2.E-14	1.E-13	2.E-13
	1.E-06	1.E-15	1.E-14	1.E-13	2.E-13	2.E-13
	1.E-05	5.E-15	5.E-14	1.E-13	2.E-13	2.E-13
	1.E-04	7.E-15	5.E-14	1.E-13	2.E-13	2.E-13
	1.E-03	7.E-15	5.E-14	1.E-13	2.E-13	2.E-13
	1.E-02	7.E-15	5.E-14	1.E-13	2.E-13	2.E-13
		Cs-135 (N=6.9 x 10^2 g)				
Degradation Rate	1.E-09	6.E-14	6.E-13	6.E-12	6.E-11	6.E-10
	1.E-08	6.E-13	6.E-12	6.E-11	6.E-10	6.E-09
	1.E-07	5.E-12	5.E-11	5.E-10	5.E-09	5.E-08
	1.E-06	2.E-11	2.E-10	2.E-09	2.E-08	2.E-07
	1.E-05	3.E-11	3.E-10	3.E-09	3.E-08	3.E-07
	1.E-04	4.E-11	4.E-10	4.E-09	4.E-08	4.E-07
	1.E-03	4.E-11	4.E-10	4.E-09	4.E-08	4.E-07
	1.E-02	4.E-11	4.E-10	4.E-09	4.E-08	4.E-07
		Se-79 (N=4.5 x 10^1 g)				
Degradation Rate	1.E-09	2.E-14	2.E-13	2.E-12	5.E-12	8.E-12
	1.E-08	2.E-13	2.E-12	5.E-12	8.E-12	8.E-12
	1.E-07	2.E-12	5.E-12	8.E-12	8.E-12	8.E-12
	1.E-06	5.E-12	8.E-12	8.E-12	8.E-12	8.E-12
	1.E-05	6.E-12	8.E-12	8.E-12	8.E-12	8.E-12
	1.E-04	6.E-12	8.E-12	8.E-12	8.E-12	8.E-12
	1.E-03	6.E-12	8.E-12	8.E-12	8.E-12	8.E-12
	1.E-02	6.E-12	8.E-12	8.E-12	8.E-12	8.E-12

Table 3.6: Safety indicators for solubility limited and sorbing nuclides.

		Inventory Factor				
		0.001	0.01	0.1	1	10
		Np-237 and Daughters (N=6.5 x 10^2 g)				
Degradation Rate	1.E-09	3.E-13	3.E-12	3.E-11	3.E-10	9.E-10
	1.E-08	3.E-12	3.E-11	3.E-10	9.E-10	9.E-10
	1.E-07	3.E-11	3.E-10	9.E-10	9.E-10	9.E-10
	1.E-06	1.E-10	8.E-10	9.E-10	9.E-10	9.E-10
	1.E-05	2.E-10	8.E-10	9.E-10	9.E-10	9.E-10
	1.E-04	2.E-10	8.E-10	9.E-10	9.E-10	1.E-09
	1.E-03	2.E-10	8.E-10	9.E-10	9.E-10	1.E-09
	1.E-02	2.E-10	8.E-10	9.E-10	9.E-10	1.E-09
		Pu and Daughters (N=4.9 x 10^3 g)				
Degradation Rate	1.E-09	4.E-15	4.E-14	4.E-13	3.E-12	2.E-11
	1.E-08	4.E-14	3.E-13	3.E-12	2.E-11	2.E-10
	1.E-07	3.E-13	2.E-12	2.E-11	2.E-10	2.E-09
	1.E-06	2.E-12	2.E-11	2.E-10	1.E-09	9.E-09
	1.E-05	4.E-12	4.E-11	4.E-10	3.E-09	1.E-08
	1.E-04	5.E-12	5.E-11	5.E-10	3.E-09	1.E-08
	1.E-03	5.E-12	5.E-11	5.E-10	3.E-09	1.E-08
	1.E-02	5.E-12	5.E-11	5.E-10	3.E-09	1.E-08
		Am and Daughters (N=2.1 x 10^3 g)				
Degradation Rate	1.E-09	3.E-13	3.E-12	3.E-11	3.E-10	9.E-10
	1.E-08	3.E-12	3.E-11	3.E-10	9.E-10	9.E-10
	1.E-07	3.E-11	3.E-10	9.E-10	9.E-10	9.E-10
	1.E-06	1.E-10	8.E-10	9.E-10	9.E-10	9.E-10
	1.E-05	2.E-10	8.E-10	9.E-10	9.E-10	9.E-10
	1.E-04	2.E-10	8.E-10	9.E-10	9.E-10	1.E-09
	1.E-03	2.E-10	8.E-10	9.E-10	9.E-10	1.E-09
	1.E-02	2.E-10	8.E-10	9.E-10	9.E-10	1.E-09
		U and Daughters (N=9.8 x 10^5 g)				
Degradation Rate	1.E-09	2.E-15	2.E-14	1.E-13	5.E-13	6.E-13
	1.E-08	2.E-14	1.E-13	5.E-13	6.E-13	7.E-13
	1.E-07	1.E-13	4.E-13	6.E-13	7.E-13	2.E-12
	1.E-06	3.E-13	6.E-13	7.E-13	1.E-12	7.E-12
	1.E-05	4.E-13	7.E-13	8.E-13	2.E-12	9.E-12
	1.E-04	4.E-13	7.E-13	9.E-13	3.E-12	9.E-12
	1.E-03	4.E-13	7.E-13	9.E-13	3.E-12	9.E-12
	1.E-02	4.E-13	7.E-13	9.E-13	3.E-12	9.E-12

Table 3.7: Safety indicators for the actinides and their daughters.

The peaks for highly soluble, non sorbing elements such as I and Cl are directly proportional to mass factor for most values of waste form degradation rates. This effect can be seen in Figures **??**, **??**, **??**, and **??**.

Highly soluble and non-sorbing ^{129}I demonstrates a direct proportionality between dose rate and fractional degradation rate until a turnover where other natural system parameters dampen transport. Highly soluble and non-sorbing ^{129}I domonstrates a direct proportionality to the inventory multiplier.

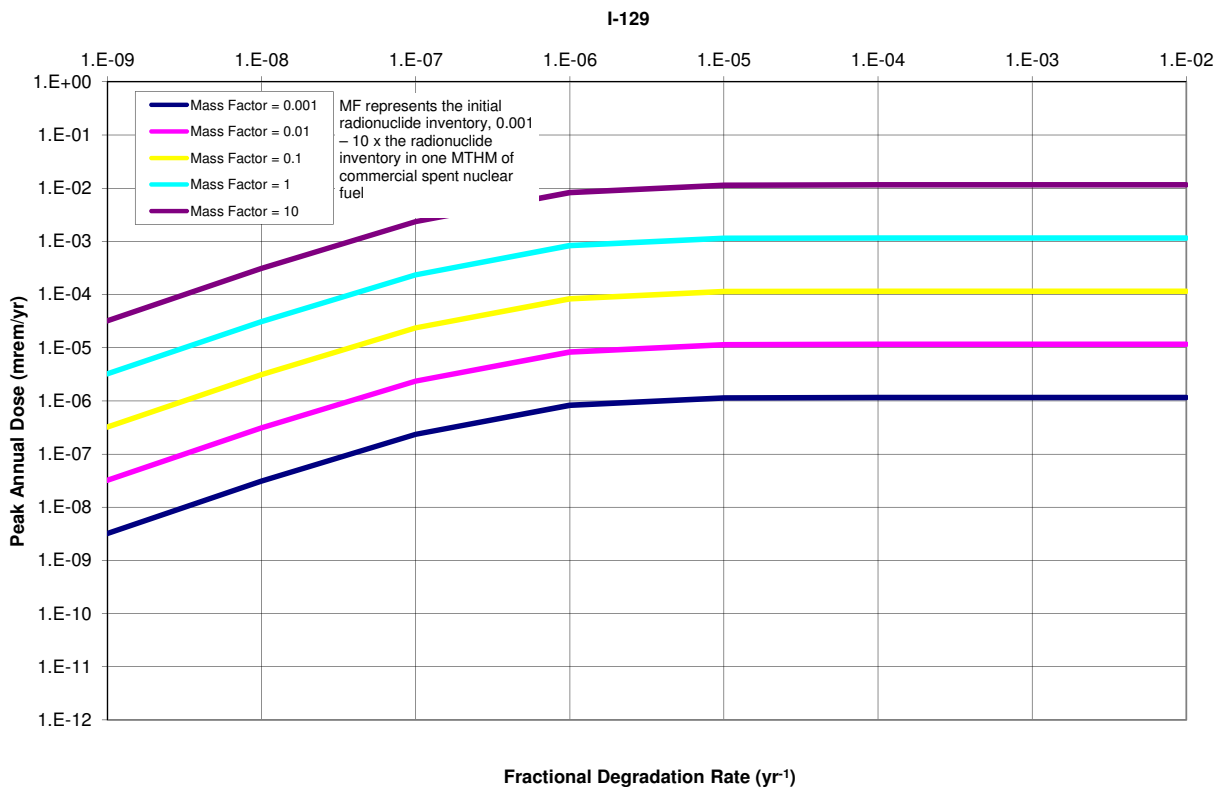

Figure 3.23: ^{129}I waste form degradation rate sensitivity.

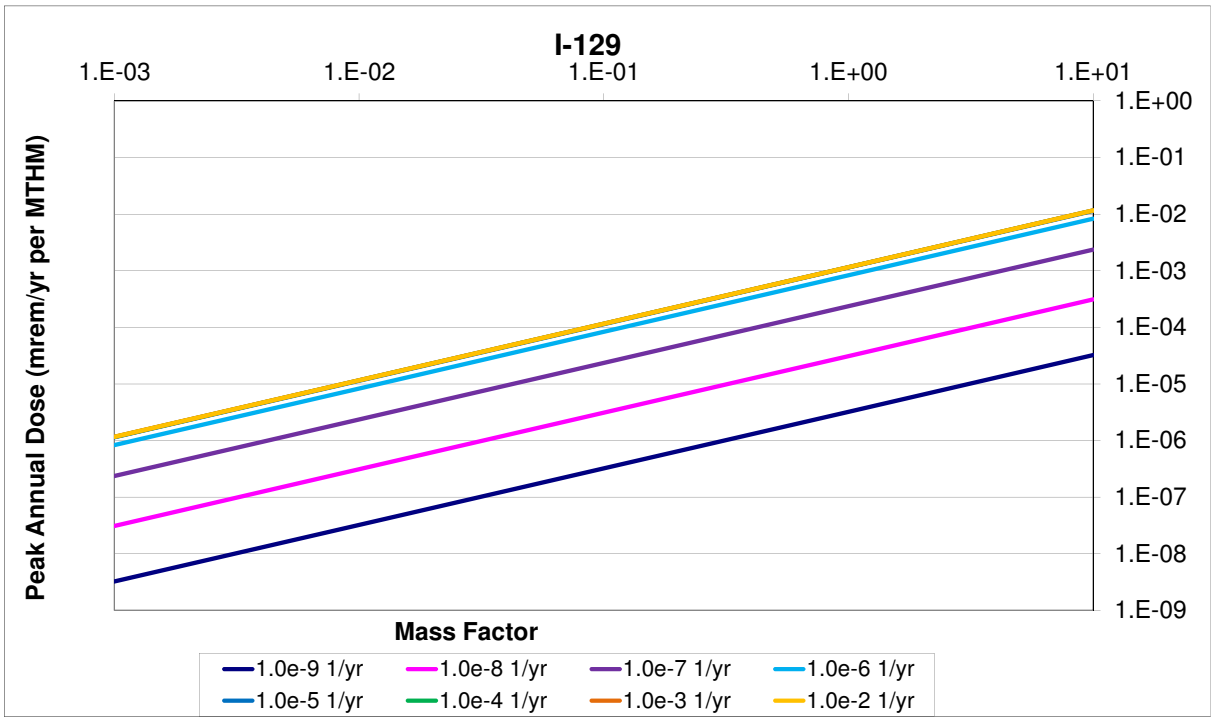

Figure 3.24: ^{129}I inventory multiplier sensitivity.

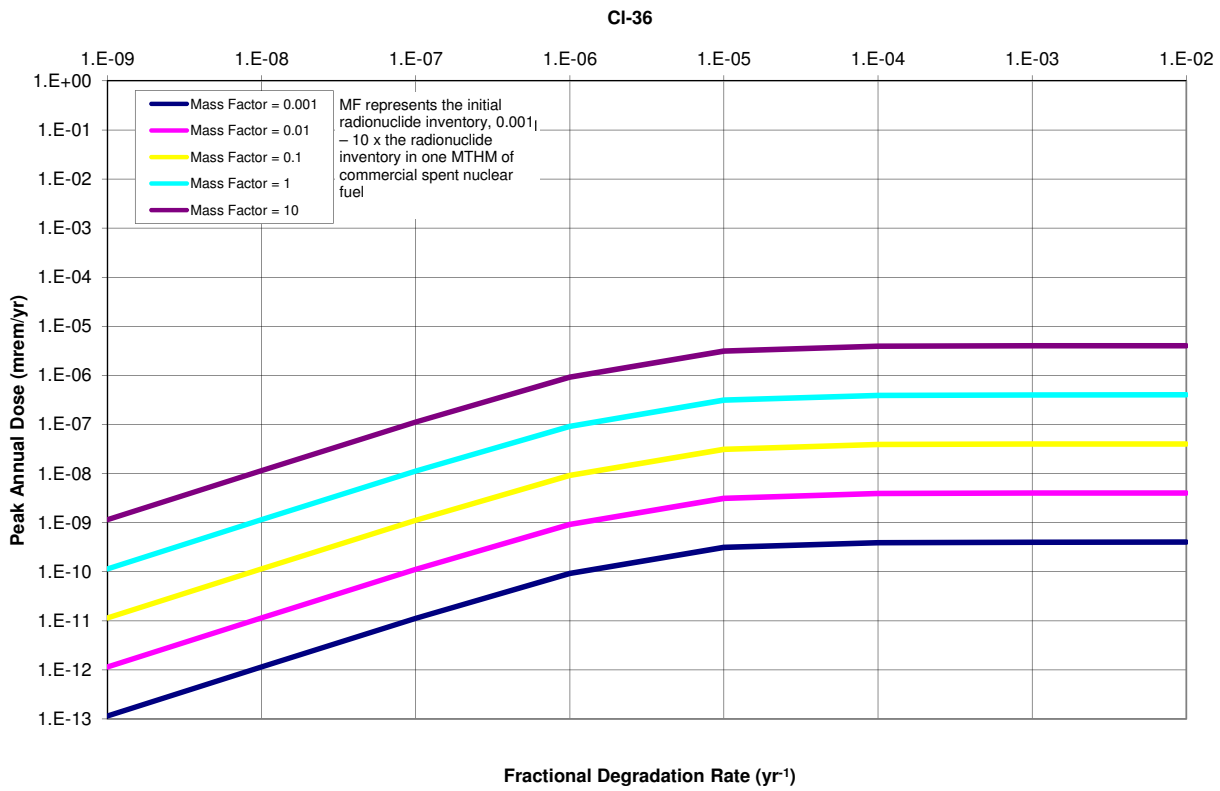

Figure 3.25: ^{36}Cl waste form degradation rate sensitivity.

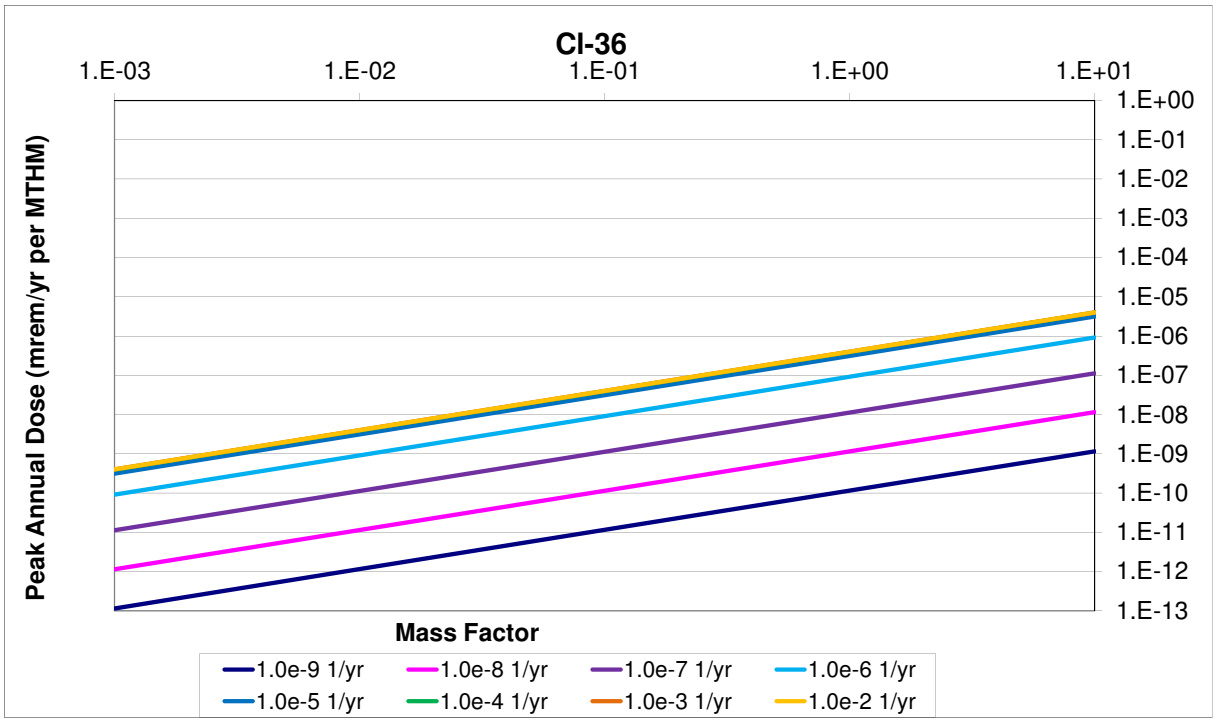

Figure 3.26: ^{36}Cl inventory multiplier sensitivity.

The peaks for solubility limited, sorbing elements such as Tc and Np, on the other hand, have a more dramatic turnover. For very high degradation rates, the dependence on mass factor starts to round off due to attenuation by solubility limits, as can be seen in Figures **??**, **??**, **??**, and **??**.

Solubility limited and sorbing ^{99}Tc demonstrates a direct proportionality to fractional degradation rate until attuation by its solubility limit and other natural system parameters.

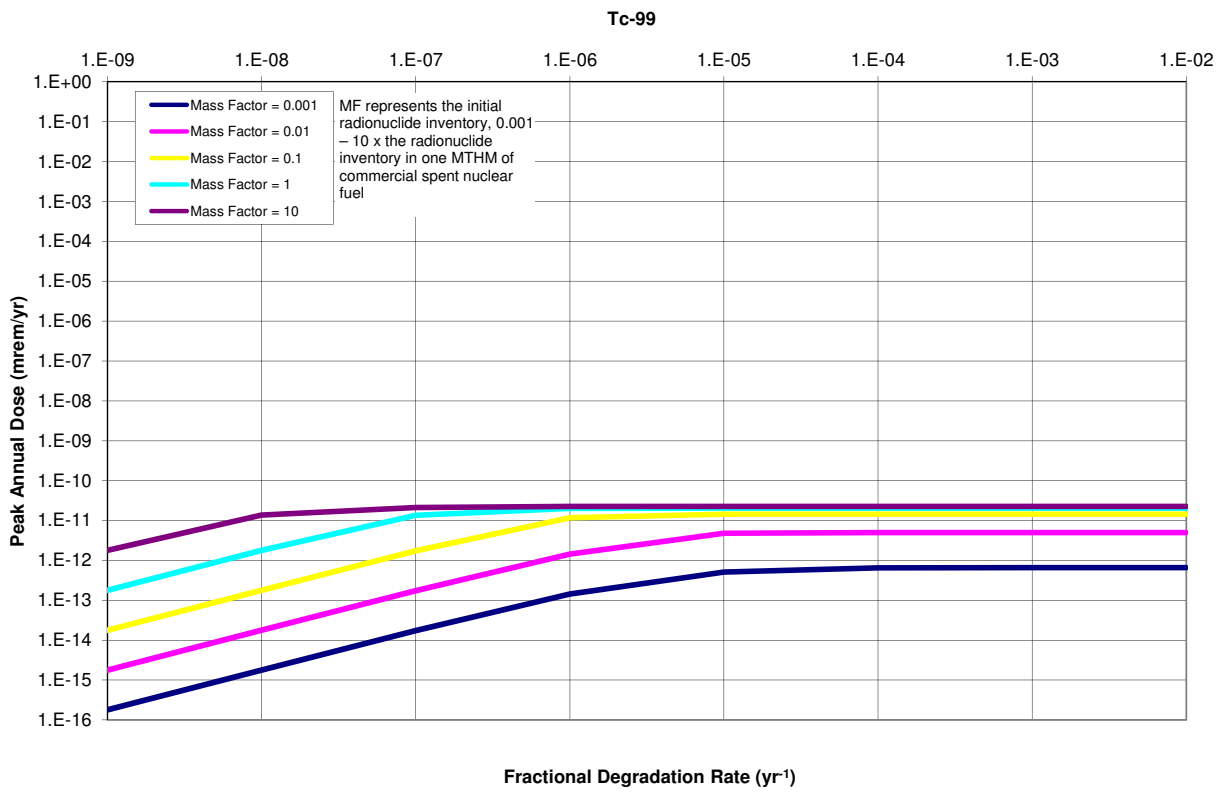

Figure 3.27: ^{99}Tc waste form degradation rate sensitivity.

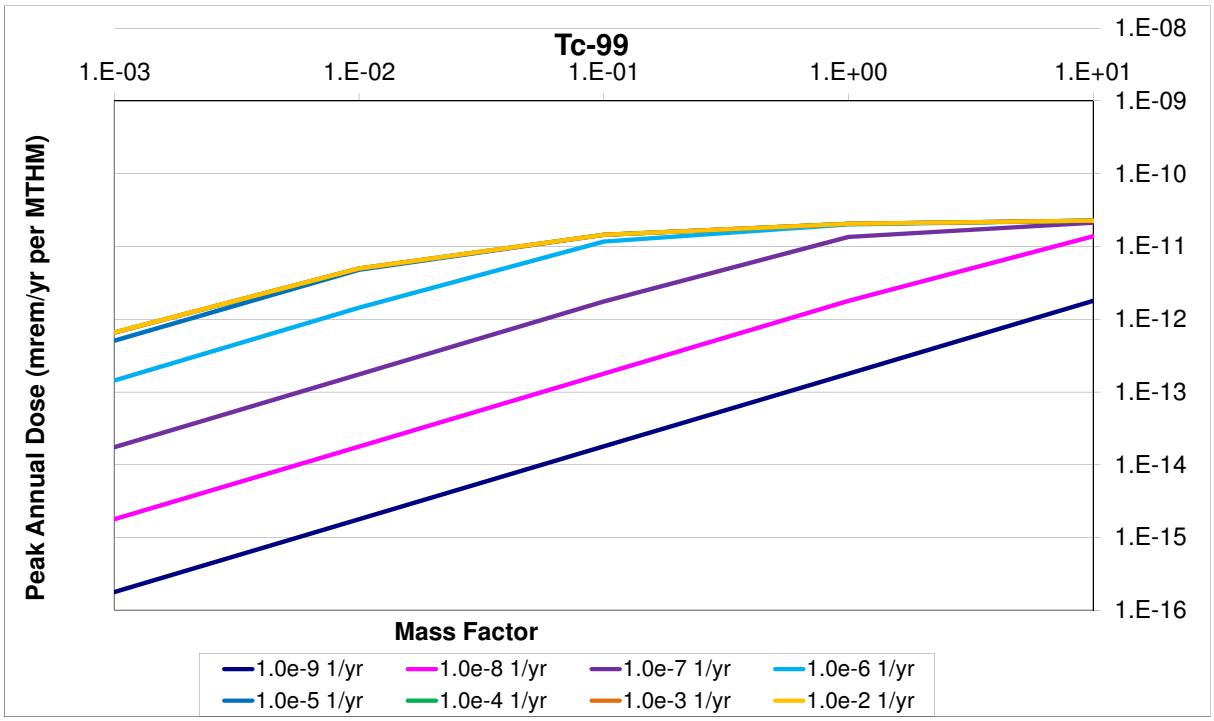

Figure 3.28: ^{99}Tc inventory multiplier sensitivity.

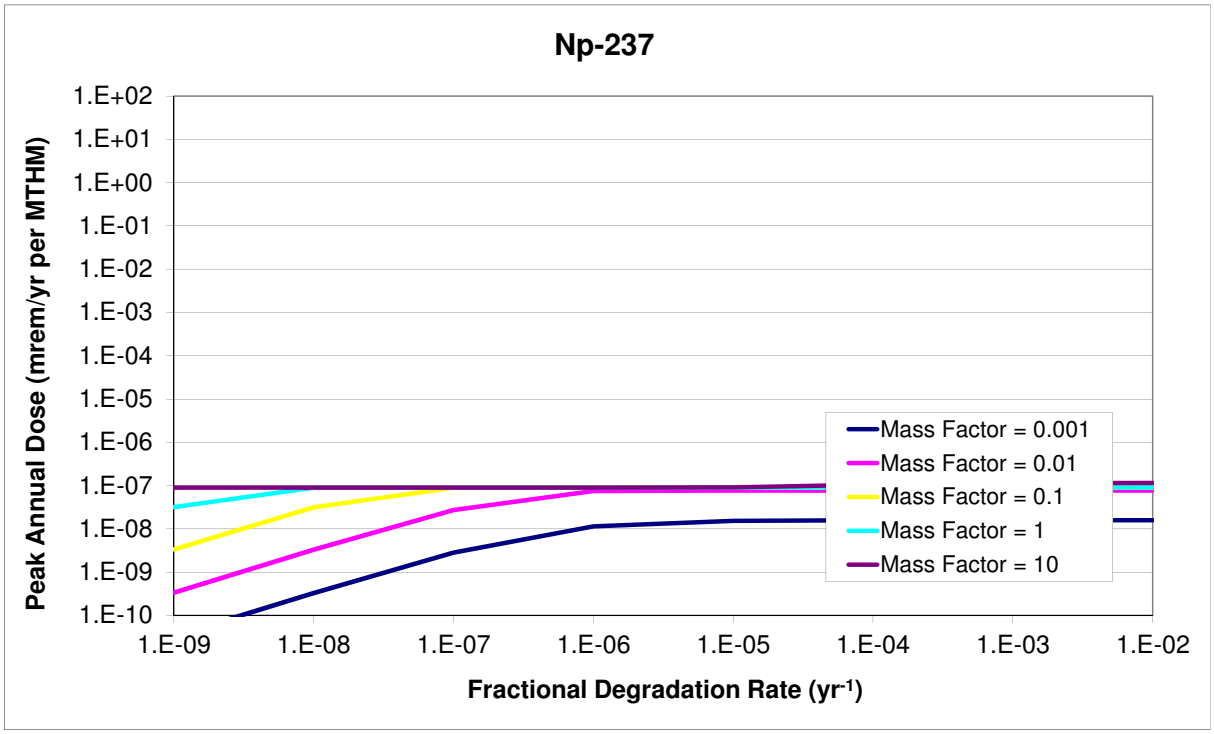

Figure 3.29: ^{237}Np waste form degradation rate sensitivity.

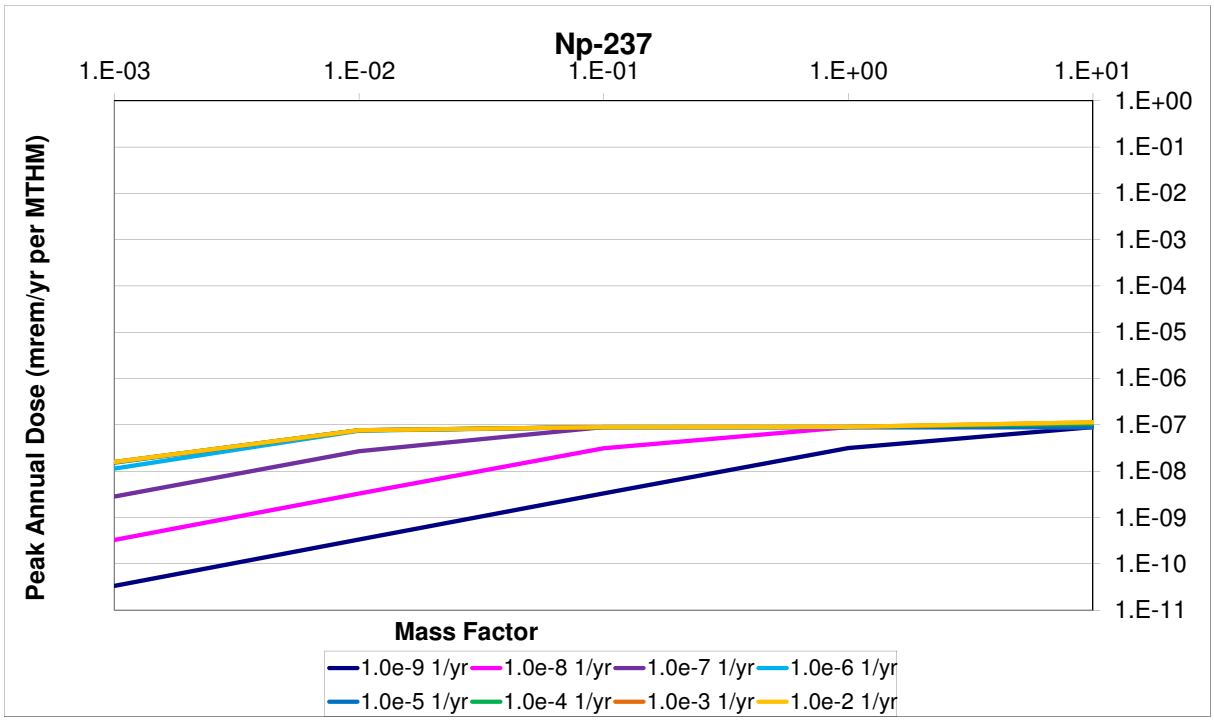

Figure 3.30: ^{237}Np inventory multiplier sensitivity.

Waste Package Failure Time

The time of waste package failure was not expected to greatly effect the magnitude of the mean of the peak doses except for cases in which waste package failure times exceeded the half lives of dominant dose-contributing nuclides. That is, since the dominant dose-contributing radionuclides for the reference case are quite long lived (^{129}I, etc.), all but the longest reasonable waste package containment lifetime is overwhelmed by the half life of the dominant radionuclides. The long time scales of radionuclide release was expected to render the the waste package lifetime irrelevant if it was shorter than a million years.

Though the model contains a unit cell-type model, it is possible to determine, in post processing, the results of a simulation with temporally heterogeneous failures among waste packages. That is, by a weighted sum of the time histories of the no-fail case and the all-fail case, it is possible to mimic a time-varying failure among the many waste packages.

Parametric Range

To investigate the effect of the waste package failure time, it was varied over five magnitudes from one thousand to ten million years. Simultaneously, the reference diffusivity was varied over the eight magnitudes between 1×10^{-8} and 1×10^{-15} in order to determine the correlation between increased radionuclide mobility and the waste package lifetime.

Results

For the clay repository, the waste package failure time is entirely irrelevant until waste package failure times reach the million or ten million year time scale.

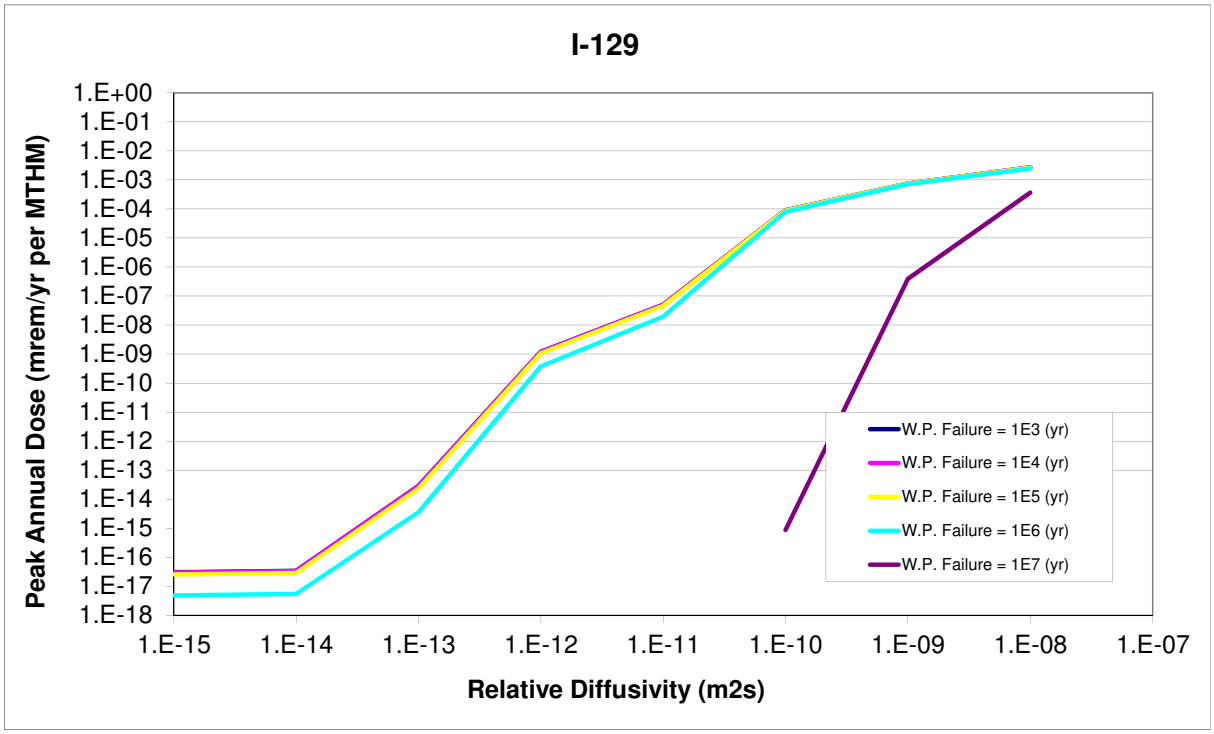

Figure 3.31: ^{129}I waste package failure time sensitivity.

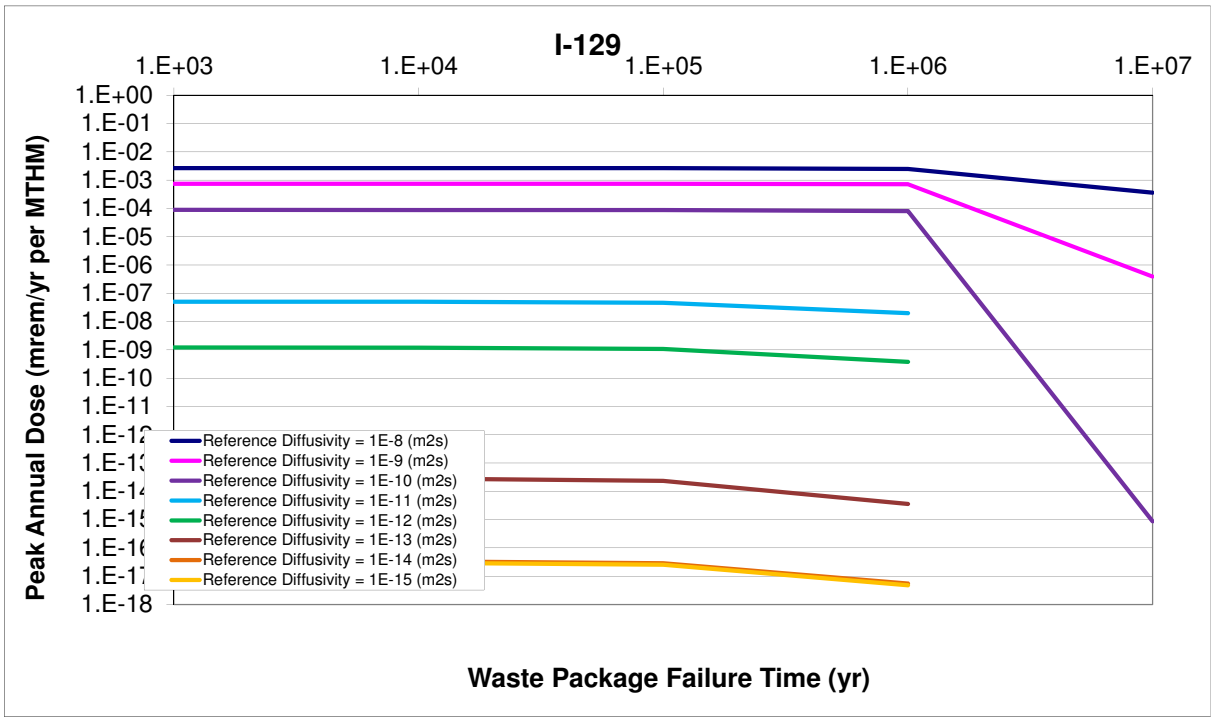

Figure 3.32: ^{129}I waste package failure time sensitivity.

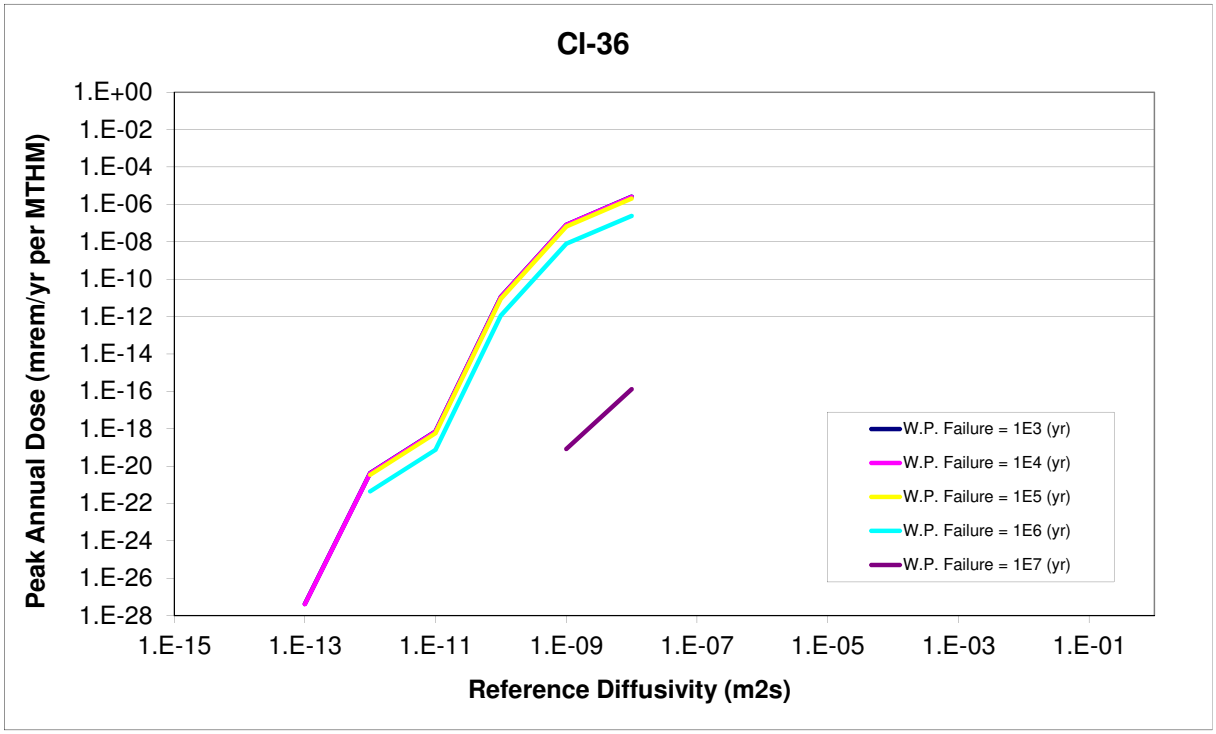

Figure 3.33: ^{36}Cl waste package failure time sensitivity.

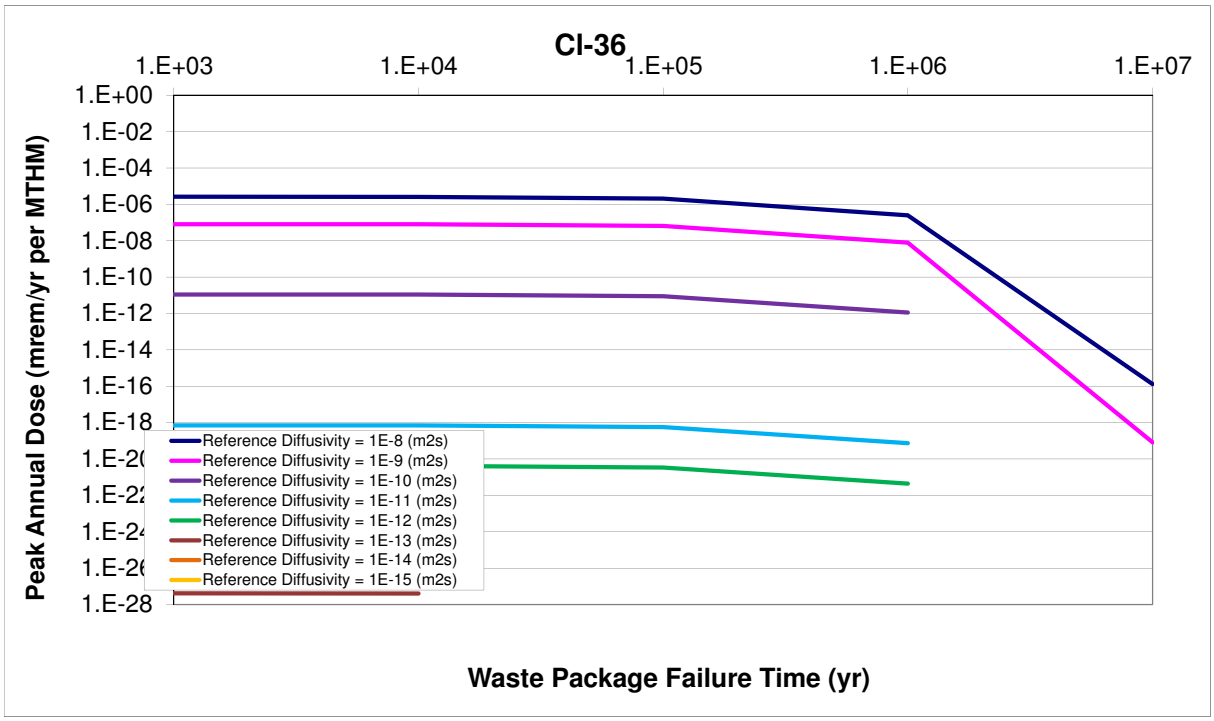

Figure 3.34: ^{36}Cl waste package failure time sensitivity.

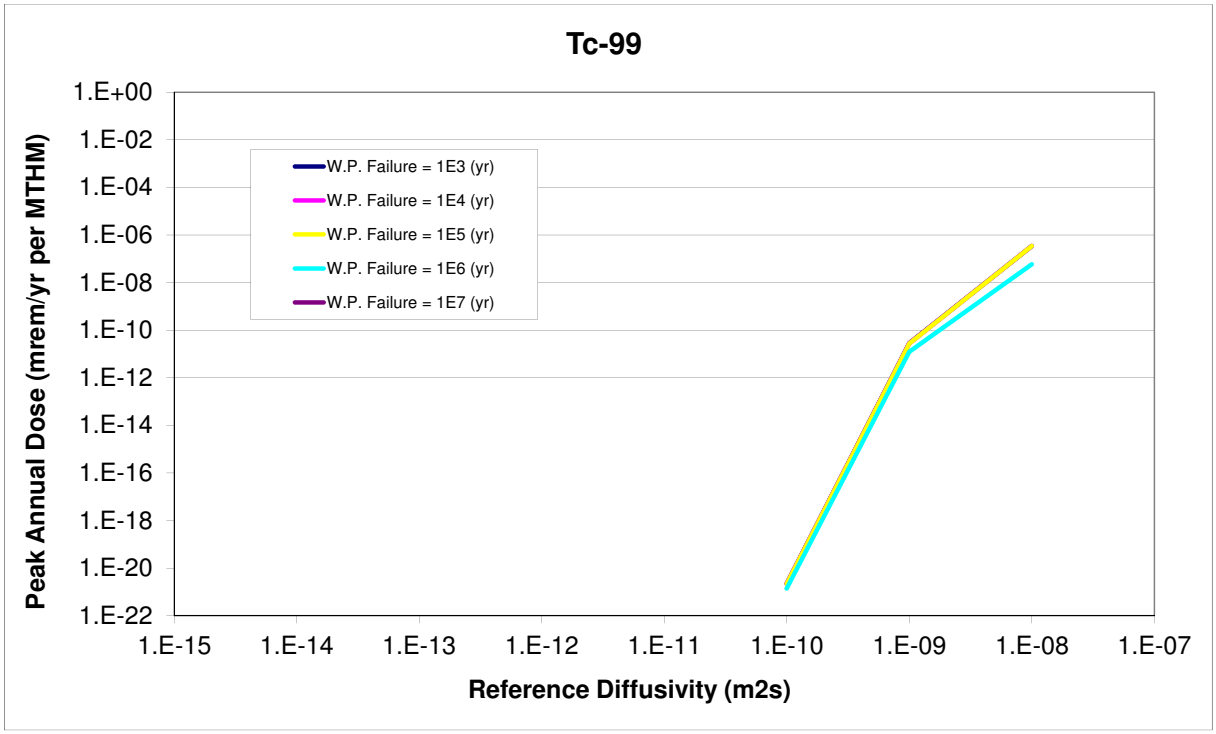

Figure 3.35: ^{99}Tc waste package failure time sensitivity.

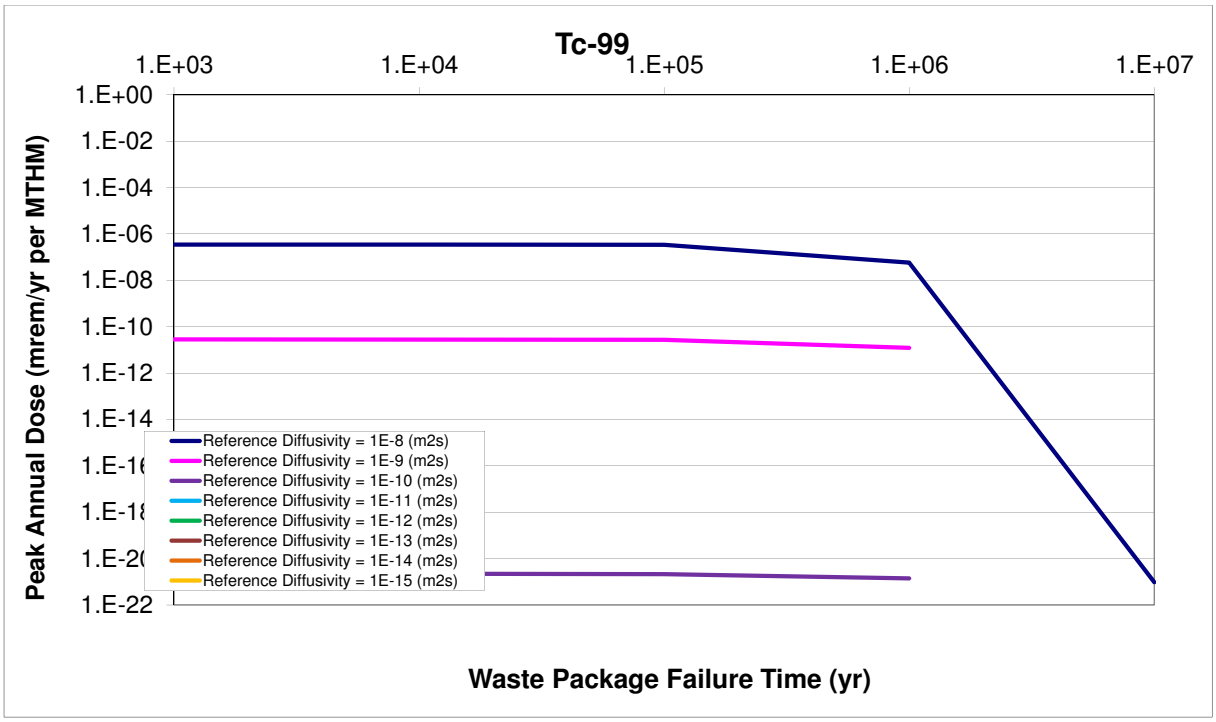

Figure 3.36: ^{99}Tc waste package failure time sensitivity.

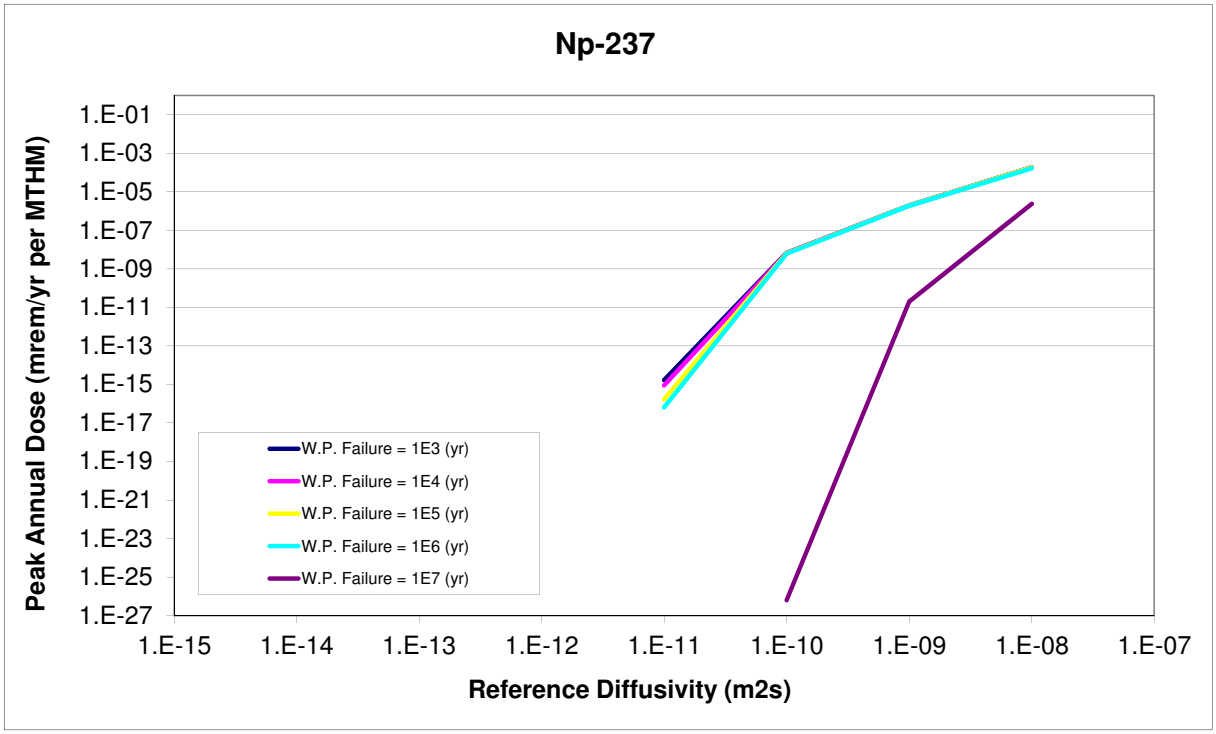

Figure 3.37: ^{237}Np waste package failure time sensitivity.

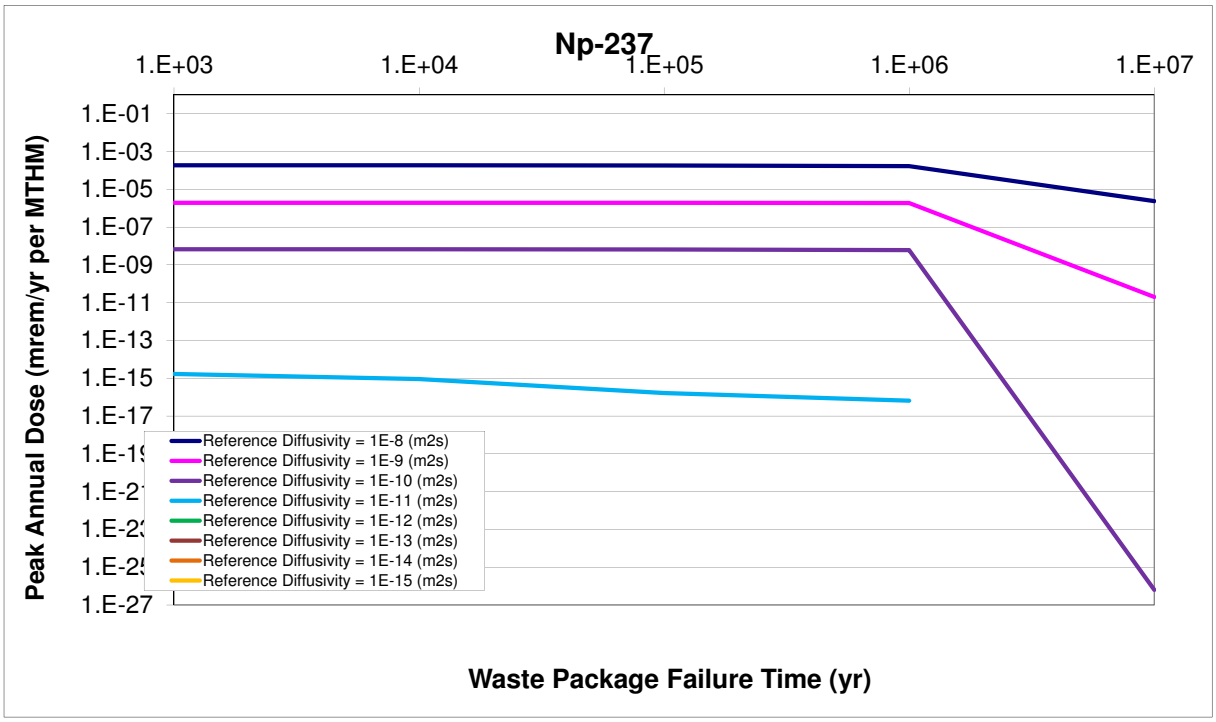

Figure 3.38: ^{237}Np waste package failure time sensitivity.

4 THERMAL TRANSPORT SENSITIVITY ANALYSIS

4.1 Isotopic Thermal Sensitivity Study

4.2 Thermal Conductivity Sensitivity Study

4.3 Diffusivity Thermal Transport Sensitivity Study

4.4 Spacing Thermal Transport Sensitivity Studies

5 COMPUTATIONAL RADIONUCLIDE TRANSPORT MODELS

Each engineered barrier component within the Generic Repository calculates nuclide transport using a model selected from those presented in this chapter. In order to be interchangeable within the simulation, these components must have identical nuclide transport interfaces.

Nuclide models may rely on a number of boundary condition forms. Each nuclide model interface must therefore provide sufficient boundary condition information to support the calculation methods of all other nuclide models. That is, each must provide a superset of the boundary condition forms used in other models. These include Dirichlet, specified species concentration along the boundary, Neumann, concentration gradients along the boundary, and Cauchy, a combination of the two that provides a concentration flux along the boundary.

For all nuclide models, mass must be conserved. Thus, all nuclide models share a mass balance paradigm.

First, since time is discrete within Cyclus , the remaining mass in a cell at the end of timestep t_n is the mass of the cell at the beginning of timestep t_{n+1}.

For all components (k) the mass balance is simply the sum over time of incoming and outgoing mass. No component has more than one external component (l), but some have many internal components (j, children). The mass balance equation for cell k is then

$$m_k^{n+1} = m_k^0 + \sum_{i=0}^{n} \left[\sum_{j=0}^{children} \left(m_{j,k}^i - m_{k,l}^i \right) \left(t_n - t_{n-1} \right) \right] \tag{5.1}$$

For a Dirichlet boundary condition, each nulcide transport model must represent a

species concentration along the boundary of the representative volume,

$$C(x, y, z, t) = C_0(x, y, z, t) \text{ for } (x, y, z) \in \Gamma \tag{5.2}$$

where

$$\begin{aligned} C(x, y, z, t) = &\text{ concentration at the boundary } [kg/m^3] \\ \Gamma = &\text{ domain boundary.} \end{aligned}$$

The second type or Neumann type boundary condition describes an impermeable boundary

$$\theta D_{ij} \frac{\partial C(x, y, z, t)}{\partial x_j} \hat{i} = 0 \text{ for } (x, y, z) \in \Gamma \tag{5.3}$$

where

$$\begin{aligned} \theta = &\text{ porosity } [-] \\ D_{ij} = &\text{ diffusion coefficient tensor component } [m^2/s]. \end{aligned}$$

The third, Cauchy, type describes a combination of the Dirichlet and Neumann type conditions, defining both a concentration at a boundary and a flux at that boundary,

$$-\theta D_{ij} \frac{\partial C}{\partial x_j} \hat{i} + q_i C \hat{i} = q_i C_0 \hat{i}. \tag{5.4}$$

where

$$q_i\hat{i} = \text{ outward fluid flux } [m/s]$$

$$\hat{i} = \text{unit vector normal to the surface } [-]$$

$$C_0 = \text{concentration of the fluid at the boundary } [kg/m^3].$$

For a Cauchy boundary condition, each nuclide transport model must represent the solute concentration flux at the outer boundary in units of $[kg/m^2/s]$. In terms of the solute mass flux, the mass balance equation is

$$m_k^{n+1} = m_k^0 + S_A \sum_{i=0}^{n} \left[\sum_{j=0}^{children} \left(\vec{J}_{j,k}^{i} - \vec{J}_{k,l}^{i} \right) (t_n - t_{n-1}) \right] \tag{5.5}$$

where

$$\vec{J}_{j,k} = \text{solute flux between j and k at time } t_i [kg/m^2/s] \tag{5.6}$$

Each component must also provide a pure source term, a mass transfer per unit time,

$$\dot{m}(x, y, z, t) = \dot{m}_0(x, y, z, t) \tag{5.7}$$

where

$$\dot{m} = \text{ mass transfer across the boundary } [kg/s].$$

For the central source cell, which has no children

$$m_0^{n+1} = m_0^0 - \sum_{i=0}^{n} m_{0,1}^n. \tag{5.8}$$

For a situation as in CYCLUS , with discrete timesteps, t_n, this becomes the available source term at the boundary between cell i and cell j at time t_n is $m_{i,j}^n$.

5.1 Degradation Rate Radionuclide Transport Model

The materials that constitute the engineered and natural barriers in a saturated repository environment degrade over time. One abstract model of the nuclide release behavior can be based solely on a fractional degradation rate. This model incorporates and source term made available on the inner boundary into its available mass and defines the resulting boundary conditions at the outer boundary as solely a function of the degradation rate of that component.

For the case in which all engineered barrier components are represented by degradation rate models, the source term at the outermost edge will be solely a function of the original central source and the degradation rates of the components. This results in the following expression for the mass transfer, $m_{ij}(t)$, from cell i to cell j at time t :

$$\dot{m}_{ij}(t) = f_i(\cdots)m_i(t) \tag{5.9}$$

where

$$\begin{aligned}
\dot{m}_{ij} &= \text{the rate of mass transfer from i to j } [kg/s] \\
f_i &= \text{fractional degradation rate } [1/s] \\
m_i &= \text{mass in cell i } [kg] \\
t &= \text{time } [s]
\end{aligned}$$

For a situation as in Cyclus , with discrete timesteps, we can assume the timesteps are small enough to assume a constant rate m_{ij} over the course of the timestep. Equation (**??**) is integrated over the timestep to give the mass transferred per timestep

$$m_{ij}^n = \int_{t_{n-1}}^{t_n} \dot{m}_{ij}(t')dt'$$

assuming a constant transfer rate

$$\begin{aligned}
&= \int_{t_{n-1}}^{t_n} f_i(\cdots)m_i^{n-1}dt' \\
&= f_i(\cdots)m_i^{n-1}\left(t_n - t_{n-1}\right). \qquad (5.10)
\end{aligned}$$

The concentration boundary condition must also be defined at the outer boundary to support parent components that utilize the Dirichlet boundary condition. For the degradation model, which incorporates no diffusion or advection, the concentration at the boundary is the average concentration in the saturated pore volume,

$$C_{ij}^n = \frac{m_i^n}{V_{vi}} \tag{5.11}$$
$$= \frac{\text{solute mass in cell i}}{\text{void volume in cell i}}.$$

To support parent components that utilize the Cauchy boundary condition, the degradation model assumes that the fluid velocity is constant across the cell as is the concentration. Thus,

$$-\theta D_{ij}\frac{\partial C}{\partial x_j}\hat{i} - \theta_i \vec{v_i} C = \theta_i^n \vec{v_0} C_0$$

$$\begin{aligned}
\theta &= \text{ porosity in cell i } [-] \\
D_{ij} &= \text{ diffusion tensor component } [m^2/s] \\
C &= \text{ concentration } [kg/m^3] \\
v_i &= \text{ velocity in i direction } [m/s]
\end{aligned}$$

reduces to

$$\theta_i \vec{v_i} C = \theta_i^n \vec{v_i^n} C_i^n. \tag{5.12}$$

5.2 Mixed Cell Volume Radionuclide Model

A main nuclide transport component model used in this work is a mixed cell component module incorporating solubility and sorption effects as well as engineered material dissolution.

A graphical representation of the mixed cell model is given in Figures **??** and **??**.

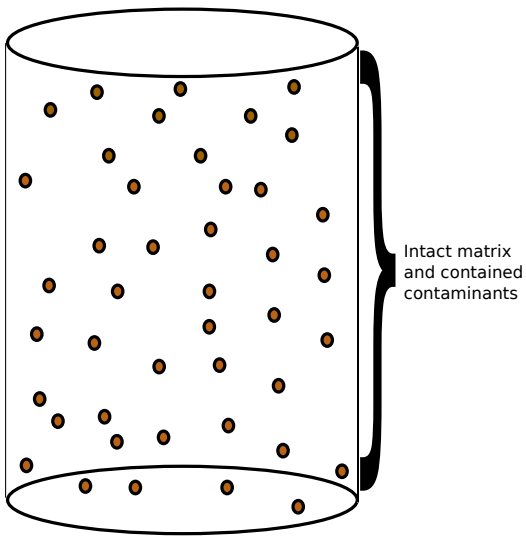

Figure 5.1: The control volume contains an intact material matrix and contaminants that are unavailable to neighboring subcomponents until dissolution has begun.

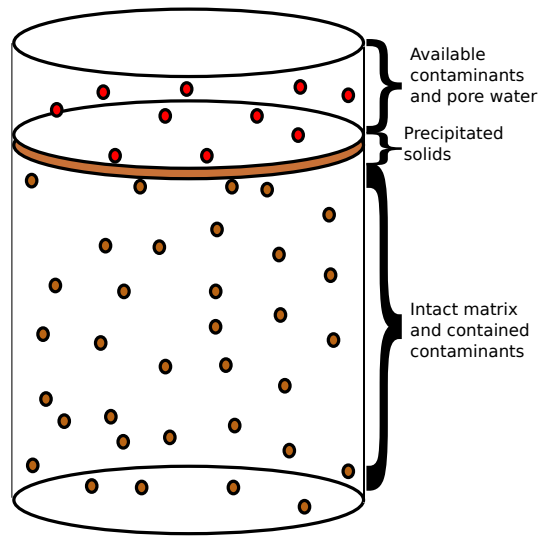

Figure 5.2: Once dissolution begins, the :control volume contains a partially dissolved material matrix, contaminated pore water, and precipitated solids.

After some time degrading, the volume of free fluid can be expressed

$$V_{ff}(t_n) = \theta V_T \int_{t_0}^{t_n} f(\cdots)dt. \tag{5.13}$$

The volume of the intact matrix can be expressed

$$V_{im}(t_n) = V_T - V_T \int_{t_0}^{t_n} f(\cdots)dt. \tag{5.14}$$

Finally, the volume of the precipitated solids can be expressed

$$V_{ps}(t_n) = (1-\theta) V_T \int_{t_0}^{t_n} f(\cdots)dt. \tag{5.15}$$

This model assumes that all net influx to the cell enters the free fluid rather than the intact matrix. The total volumetric contaminant concentration in the intact matrix, can be expressed

$$C_{im}(t_n) = C_0 \tag{5.16}$$

$$= \frac{m_0}{V_{im}} \tag{5.17}$$

where

$$m_0 = \text{ total initial mass}$$

The resulting contaminant mass in the intact matrix is

$$\begin{aligned} m_{im}(t_n) &= C_0 V_{im}(t_n) \\ &= C_0(1-\theta)V_T \int_{t_0}^{t_n} f(\cdots)dt. \end{aligned} \tag{5.18}$$

The contaminant mass in the free fluid is just the pore water concentration times the free fluid volume plus the time integral of net influx to the cell.

$$C_{ffT}(t_n) = \left[C_0 + \frac{\int_{t_0}^{t_n} \dot{m}_i(t')dt'}{V_{ff}(t_n)} \right] \tag{5.19}$$

and

$$
\begin{aligned}
m_{ffT}(t_n) &= C_{ff}(t_n)\theta V_{ff}(t_n) \\
&= \left[C_0 + \frac{\int_{t_0}^{t_n} \dot{m}_i(t')dt'}{V_{ff}(t_n)} \right] V_{ff}(t_n) \\
&= C_0 V_{ff}(t_n) + \int_{t_0}^{t_n} \dot{m}_i dt'
\end{aligned} \tag{5.20}
$$

It is limited, however, by both solubility limitation and sorption.

Sorption

The mass in both the free fluid and in the intact matrix exists in both sorbed and nonsorbed phases. The relationship between the sorbed mass concentration in the solid phase (e.g. the pore walls),

$$
s = \frac{\text{mass of sorbed contaminant}}{\text{mass of total solid phase}} \tag{5.21}
$$

and the dissolved liquid concentration,

$$
c = \frac{\text{mass of dissolved contaminant}}{\text{volume of total liquid phase}} \tag{5.22}
$$

can be expressed by a number of isotherm models.

In this model, sorption is taken into account throughout the volume. In the intact matrix, the contaminant mass is distributed between the pore walls and the pore fluid by sorption. So too, contaminant mass released from the intact matrix by degradation is distributed between dissolved mass in the free fluid and sorbed mass in the precipitated

solids.

Boundary Conditions

To solve for the boundary condiitons in this model, the amount of dissolved mass in the free fluid must be found. This value, m_{ffl}, can be expressed in terms of the total degraded contaminant mass and the contaminant mass in the precipitated solid,

$$m_{ffl} = m_{ffT} - m_{psc} \tag{5.23}$$

The mass of contaminant sorbed into the precipitated solids can be found using a linear isotherm model, characterized by the relationship

$$s_i = K_{di} c_i \tag{5.24}$$

where

$$\begin{aligned} s_i &= \text{ the solid concentration of isotope i } [kg/kg] \\ K_{di} &= \text{ the distribution coefficient of isotope i}[] \\ c_i &= \text{ the liquid concentration of isotope i } [kg/m^3]. \end{aligned}$$

Thus,

$$
\begin{aligned}
s_{i,ps} &= \frac{\text{contaminant mass in precipitated solids}}{\text{total mass of precipitated solids}} \\
&= \frac{m_{psc}}{m_{pst}} \\
&= \frac{m_{psc}}{m_{psm} + m_{psc}}
\end{aligned}
$$

where

$$
\begin{aligned}
m_{psm} &= \text{ noncontaminant mass in precipitated solids } [kg] \\
&= \rho_b V_{ps} \\
m_{psc} &= \text{ contaminant mass in precipitated solids } [kg] \\
m_{psm} &= \rho_b V_{ps}. \qquad (5.25)
\end{aligned}
$$

The following expression results, giving contaminant mass in the precipitated solids in terms of the sorption coefficient,

$$
\begin{aligned}
m_{psc} &= s_{ps} m_{psT} \\
&= K_d C_{ffl} m_{psT} \\
&= \frac{K_d m_{ffl} m_{psT}}{V_{ff}} \\
&= \frac{K_d}{V_{ff}} (m_{ffT} - m_{psc}) m_{psT} \\
&= \frac{K_d}{V_{ff}} (m_{ffT} - m_{psc})(m_{psm} + m_{psc}) \\
&= \frac{K_d}{V_{ff}} (m_{ffT} m_{psm} - m_{psc} m_{psm} + m_{ff} m_{psc} - m_{psc}^2) \\
&= \frac{K_d}{V_{ff}} (m_{ffT} m_{psm} + (m_{ffT} - m_{psm}) m_{psc} - m_{psc}^2)
\end{aligned}
$$

which, rearranged, becomes

$$0 = m_{psc}^2 + \left(-m_{ffT} + m_{psm} + \frac{V_{ff}}{K_d}\right) m_{psc} - m_{ffT} m_{psm}$$

and is solved using the quadratic formula, such that

$$\begin{aligned} m_{psc} &= \frac{m_{ffT} - m_{psm} - \frac{V_{ff}}{K_d}}{2} \\ &\pm \frac{\sqrt{m_{ffT}^2 + m_{psm}^2 + \frac{V_{ff}^2}{K_d^2} + 2m_{ffT}m_{psm} - \frac{2V_{ff}m_{ffT}}{K_d} + \frac{2V_{ff}m_{psm}}{K_d}}}{2} \end{aligned}$$

which, again rearranged, becomes

$$\begin{aligned} &= \frac{1}{2}\left(m_{ffT} - m_{psm} - \frac{V_{ff}}{K_d}\right) \\ &\pm \frac{1}{2}\sqrt{m_{ffT}^2 + 2m_{ffT}\left(m_{psm} - \frac{V_{ff}}{K_d}\right) + \left(m_{psm} + \frac{V_{ff}}{K_d}\right)^2}. \end{aligned} \tag{5.26}$$

If we plug Equation (**??**) into Equation (**??**), we arrive at the following expression for m_{ffl} in terms of known quantities

$$\begin{aligned} m_{ffl} &= m_{ffT} - \frac{1}{2}\left(m_{ffT} - m_{psm} - \frac{V_{ff}}{K_d}\right) \\ &\mp \frac{1}{2}\sqrt{m_{ffT}^2 + 2m_{ffT}\left(m_{psm} - \frac{V_{ff}}{K_d}\right) + \left(m_{psm} + \frac{V_{ff}}{K_d}\right)^2}. \end{aligned} \tag{5.27}$$

We can express the desired boundary conditions in terms of m_{ffl}. First, the Dirichlet

boundary condition is

$$C(x, y, z, t) = \frac{m_{ffl}(t)}{V_{ff}(t)} \forall (x, y, x) \in \Gamma. \tag{5.28}$$

Again, the concentration gradient can be specified across the boundary only with reference to the concentration at a point external to the component. If the concentration C_{ext} is specified at a location r_{ext}, the Neumann condition is a function of those concentrations, $C(x, y, z, t)$, and a corresponding location inside the component. If we choose radius furthest from either wall of the inner component, r_c,

$$\frac{\partial C}{\partial r} = \frac{C_{ext} - C(x, y, z, t)}{r_{ext} - r_c} \tag{5.29}$$

such that

$$\theta_i \vec{v_i}(t) C(x, y, z, t) \frac{C_{ext} - C(x, y, z, t)}{r_{ext} - r_c} = \theta_i \vec{v_i}(t) C(x, y, z, t). \tag{5.30}$$

5.3 Lumped Parameter Radionuclide Model

5.4 One Dimensional Permeable Porous Medium Radionuclide Transport Model

Various solutions to the advection dispersion equation in Equation (**??**) have been published for both the first and third types of boundary conditions. The third, Cauchy type, is mass conservative, and will be the primary kind of boundary condition used at the source for this model.

One Dimensional Semi-Infinite Solution

The conceptual model in Figure **??** represents solute transport in one dimension with unidirectional flow and a semi-infinite boundary condition in the positive flow direction.

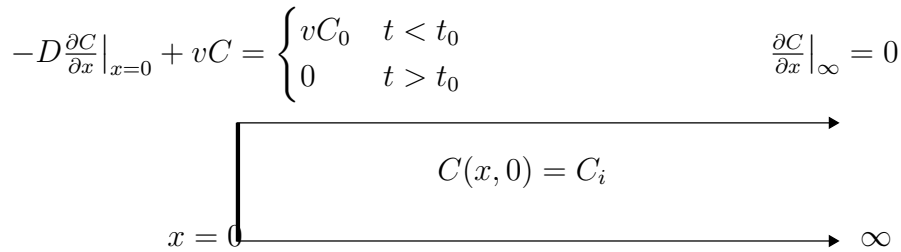

Figure 5.3: Case I, a one dimensional, semi-infinite model.

With the boundary conditions

$$-D\frac{\partial C}{\partial x}\big|_{x=0} + v_x c = \begin{cases} vC_0 & (0 < t < t_0) \\ 0 & (t > t_0) \end{cases} \tag{5.31}$$

$$\frac{\partial C}{\partial x}\big|_{x=\infty} = 0 \tag{5.32}$$

and the initial condition

$$C(x,0) = C_i, \tag{5.33}$$

the solution is given as

$$C(x,t) = \begin{cases} C_i + (C_0 - C_i)\, A(x,t) & 0 < t < t_0 \\ C_i + (C_0 - C_i)\, A(x,t) - C_0 A(x, t - t_0) & t > t_0 \end{cases} \tag{5.34}$$

where

$$A(x,t) = \frac{1}{2}\,\mathrm{erfc}\left[\frac{Rx - vt}{2\sqrt{DRt}}\right] + \sqrt{\frac{v^2 t}{\pi D R}}\, e^{-\frac{(Rx-vt)^2}{4DRt}}. \tag{5.35}$$

One Dimensional Semi-Infinite Solution with Discrete Source

The conceptual model in Figure **??** represents solute transport in one dimension with unidirectional flow and a semi-infinite boundary condition in the positive flow direction.

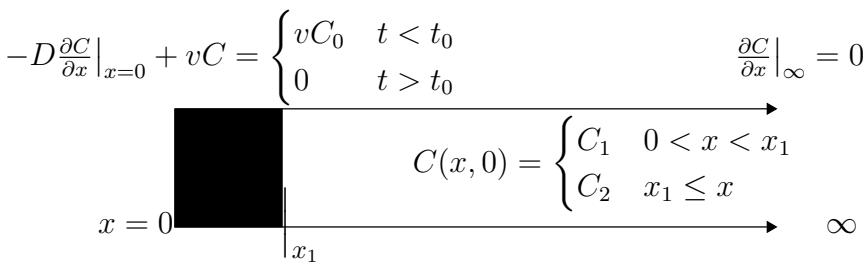

Figure 5.4: Case II, a one dimensional, semi-infinite model.

With the boundary conditions

$$-D\frac{\partial C}{\partial x}\Big|_{x=0} + v_x c = \begin{cases} vC_0 & (0 < t < t_0) \\ 0 & (t > t_0) \end{cases} \tag{5.36}$$

$$\frac{\partial C}{\partial x}\Big|_{x=\infty} = 0 \tag{5.37}$$

and the initial condition

$$C(x,0) = C_i, \tag{5.38}$$

the solution is given as

$$C(x,t) = \begin{cases} C_i + (C_0 - C_i)\, A(x,t) & 0 < t < t_0 \\ C_i + (C_0 - C_i)\, A(x,t) - C_0 A(x, t - t_0) & t > t_0 \end{cases} \tag{5.39}$$

where

$$A(x,t) = \frac{1}{2}\,\mathrm{erfc}\left[\frac{Rx - vt}{2\sqrt{DRt}}\right] + \sqrt{\frac{v^2 t}{\pi D R}} e^{-\frac{(Rx-vt)^2}{4DRt}}. \tag{5.40}$$

One Dimensional Finite Solution

The conceptual model in Figure **??** represents solute transport in one dimension with unidirectional flow and a finite boundary condition in the positive flow direction.

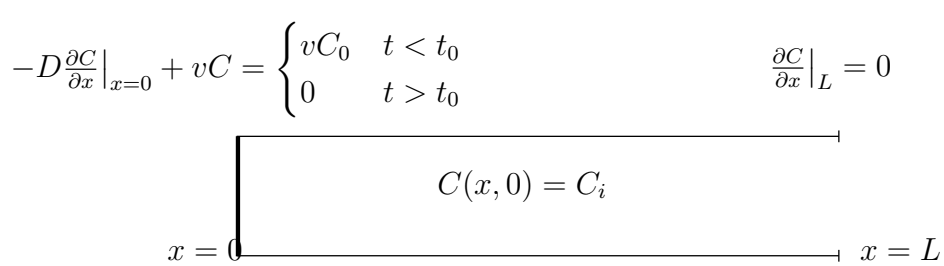

Figure 5.5: Case III, a one dimensional, finite model.

With the boundary conditions

$$-D\frac{\partial C}{\partial x}\Big|_{x=0} + v_x c = \begin{cases} vC_0 & (0 < t < t_0) \\ 0 & (t > t_0) \end{cases} \tag{5.41}$$

$$\frac{\partial C}{\partial x}\Big|_{x=L} = 0 \tag{5.42}$$

and the initial condition

$$C(x,0) = C_i, \tag{5.43}$$

the solution is given as

$$C(x,t) = \begin{cases} C_2 + (C_1 - C_2)\, A(x,t) + (C_0 - C_1)\, B(x,t) & 0 < t < t_0 \\ C_2 + (C_1 - C_2)\, A(x,t) + (C_0 - C_1)\, B(x,t) - C_0 B(x, t - t_0) & 0 < t < t_0 \end{cases} \tag{5.44}$$

where

$$\begin{aligned} A(x,t) = {} & \frac{1}{2}\operatorname{erfc}\left[\frac{R(x-x_1) - vt}{2\sqrt{DRt}}\right] + \sqrt{\frac{v^2 t}{\pi DR}} e^{\left[\frac{vx}{D} - \frac{R}{4Dt}(x + x_1 + \frac{vt}{R})^2\right]} \\ & - \frac{1}{2}\left[1 + \frac{v(x+x_1)}{D} + \frac{v^2 t}{DR}\right] e^{\frac{vx}{D}} \operatorname{erfc}\left[\frac{R(x+x_1) + vt}{2\sqrt{DRt}}\right] \end{aligned} \tag{5.45}$$

$$\begin{aligned} B(x,t) = {} & \frac{1}{2}\operatorname{erfc}\left[\frac{Rx - vt}{2\sqrt{DRt}}\right] + \sqrt{\frac{v^2 t}{\pi DR}} e^{-\left[\frac{(Rx - vt)^2}{4DRt}\right]} \\ & - \frac{1}{2}\left[1 + \frac{vx}{D} + \frac{v^2 t}{DR}\right] e^{\frac{vx}{D}} \operatorname{erfc}\left[\frac{Rx + vt}{2\sqrt{DRt}}\right]. \end{aligned} \tag{5.46}$$

6 THERMAL TRANSPORT COMPUTATIONAL MODELS

6.1 Thermal Capacity Approximation Methodology

6.2 Lumped Parameter Thermal Transport Computational Model

7 SYSTEM LEVEL ANALYSIS OF THE GENERIC REPOSITORY MODEL

8 COMPONENT ANALYSIS OF THE GENERIC REPOSITORY MODEL

9 CONCLUSIONS AND FUTURE WORK